

Introduction to surface & interface

1. Introduction to lecture (syllabus)
2. Introduction to surface and interface

Reading: Kolasinski, Introduction

2019 Spring

458-622 Advanced Surface Chemistry, 표면화학특론

LECTURER: Professor Yung-Eun Sung (성영은)

Office: Rm #729, Phone: 880-1889, E-mail: ysung@snu.ac.kr

homepage: <http://pin.snu.ac.kr/~peel>

OUTLINE

This class deals with basic principles of surface and interface at solid and liquid. Those include structures and adsorbates, experimental techniques, thermodynamics & kinetics on surface, liquid interfaces, and application to catalysis, electrocatalysis, and nanoscience.

TEXTBOOKS

Kurt W. Kolasinski, Surface Science – Foundations of Catalysis and Nanoscience (3rd edition), Wiley. 2012. (old Versions are all right.)

REFERENCES

G. A. Somorjai, Introduction to Surface Chemistry and Catalysis, John Wiley.
(e-Book available in SNU Library)

Duncan J. Shaw, Introduction to Colloid and Surface Chemistry, John Wiley.
(Korean reference: 임재석, 임평, 콜로이드과학 및 표면화학, 내하출판사, 2015)

SCHEDULES

1. Introduction to Surface & Interface (Introduction) (1 week)
2. Surface and Adsorbate Structure (ch.1) (1-2 weeks)
3. Experimental Probes and Techniques (ch.2) (3-4 weeks)
4. Chemisorption, Physisorption and Dynamics (ch.3) (5-6 weeks)
5. Thermodynamics and Kinetics of Adsorption and Desorption (ch.4) (7-8 weeks)
6. Thermodynamics of Surface and Interface (ch.5) (9-10 weeks)
7. Liquid Interfaces (ch.5) (11-13 weeks)
8. Application to Catalysis and Nanoscience (ch.6, 7, 8) (14-15 week)

GRADING ($\geq B^+$ <80%) Midterm Exam 40%, Final Exam 40%, Homeworks & Attendance 20 %

LECTURE ROOM & TIME: Rm #302-720, 12:30-13:45 Mon. & Wed.

OFFICE HOUR: Rm #302-729, 14:00-17:00 Mon. & Wed.

TA: Min Her(허민), Rm 311-217(ICP), 880-1587, 010-3139-0781, her9305@snu.ac.kr

History of surface science

Early 1800s

- Spontaneous spreading of oil on water: Benjamin Franklin
- Platinum-surface-catalyzed reaction of H_2 & O_2 in 1823 (Dobereiner): portable flame (“lighter”)
- Discovery of heterogeneous catalysis by 1835: Kirchhoff, Davy, Henry, Philips, Faraday, Berzelius
- Photography by 1835: Daguerre process
- Study of tribology or friction by this time

1860-1912

- Surface-catalyzed chemistry-based technologies: Deacon process ($2\text{HCl} + \text{O}_2 \rightarrow \text{H}_2\text{O} + \text{Cl}_2$), SO_2 oxidation to SO_3 (Messel, 1875), CH_4 reaction with steam to CO & H_2 (Mond, 1888), NH_3 oxidation (Ostwald, 1901), C_2H_4 hydrogenation (Sabatier, 1902), NH_3 synthesis (Haber, Mittasch, 1905-12)
- Surface tension measurement \rightarrow thermodynamics of surface phases (Gibbs, 1877)
- Colloids (Graham, 1861), micelles (Nageli), metal colloids (Faraday) \rightarrow paint industry, artificial rubber in early 20th century

Early 20th century

- Light bulb filament, high-surface-area gas absorbers in the gas mask, gas-separation technologies → atomic & molecular adsorption (Langmuir, 1915)
- Studies of electrode surface in electrochemistry (from 19th century)
- Surface diffraction of electrons (Davisson & Germer, 1927)
- Surface studies: Germany (Haber, Polanyi, Farkas, Bonhoefer), UK (Rideal, Roberts, Bowden), USA (Langmuir, Emmett, Harkins, Taylor, Ipatief, Adams), and other countries

After 1950s & 2000s

- Gas-phase molecular process on the molecular level
- Ultra high vacuum (UHV) system
- Surface characterization techniques
- Scanning tunneling microscope (STM, Binnig & Rohrer, 1983) (Nobel Prize in 1986): atomic scale image & manipulation
- Graphene (Novoselov & Geim, 2004) (Nobel Prize in 2010)
- Nobel Prize in 2007 to Gerhard Ertl for “chemical processes on solid surfaces”
- Nanotechnology in 2000’s

Surfaces and interfaces

- Surface: interface between immiscible bodies
- Outer space: solid-vacuum interface
- Surfaces on earth are exposed to another solid or gas or liquid → interface: s/s , s/l , s/g , l/l , l/g

Interfaces

- On earth, surfaces are always covered with a layer of atoms or molecules → interfaces

s/g, s/l, l/l, s/s/ l/g

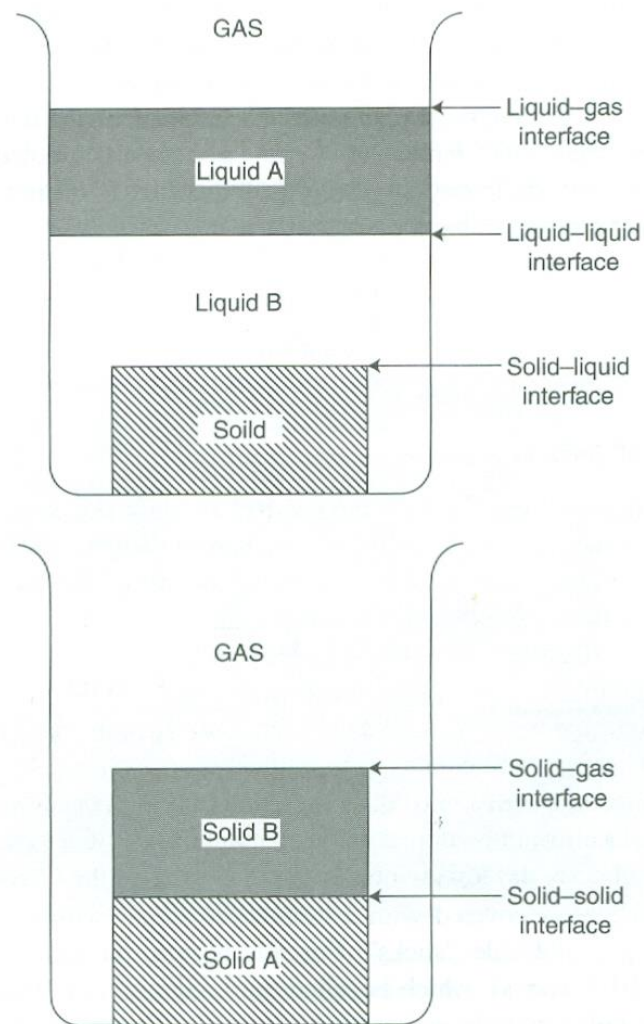


Figure 1.12. Schematic diagram of interfaces (e.g., solid-liquid, liquid-liquid, liquid-gas, solid-solid, and solid-gas interfaces).

External surfaces

- Surface concentration \rightarrow estimated from the bulk density

molecular density per cm^3 , $\rho \rightarrow$ surface concentration per cm^2 , $\sigma = \rho^{2/3}$
e.g., $1 \text{ g/cm}^3 \rightarrow \rho \sim 5 \times 10^{22} \rightarrow \sigma \sim 10^{15} \text{ molecules cm}^{-2}$

- Clusters and small particles

Dispersion

$$D = \frac{\text{number of surface atoms}}{\text{total number of atoms}} \quad (1.1)$$

volume of cluster $\sim d^3$, surface area $\sim d^2 \rightarrow D \sim 1/d$ (inverse of the cluster size)

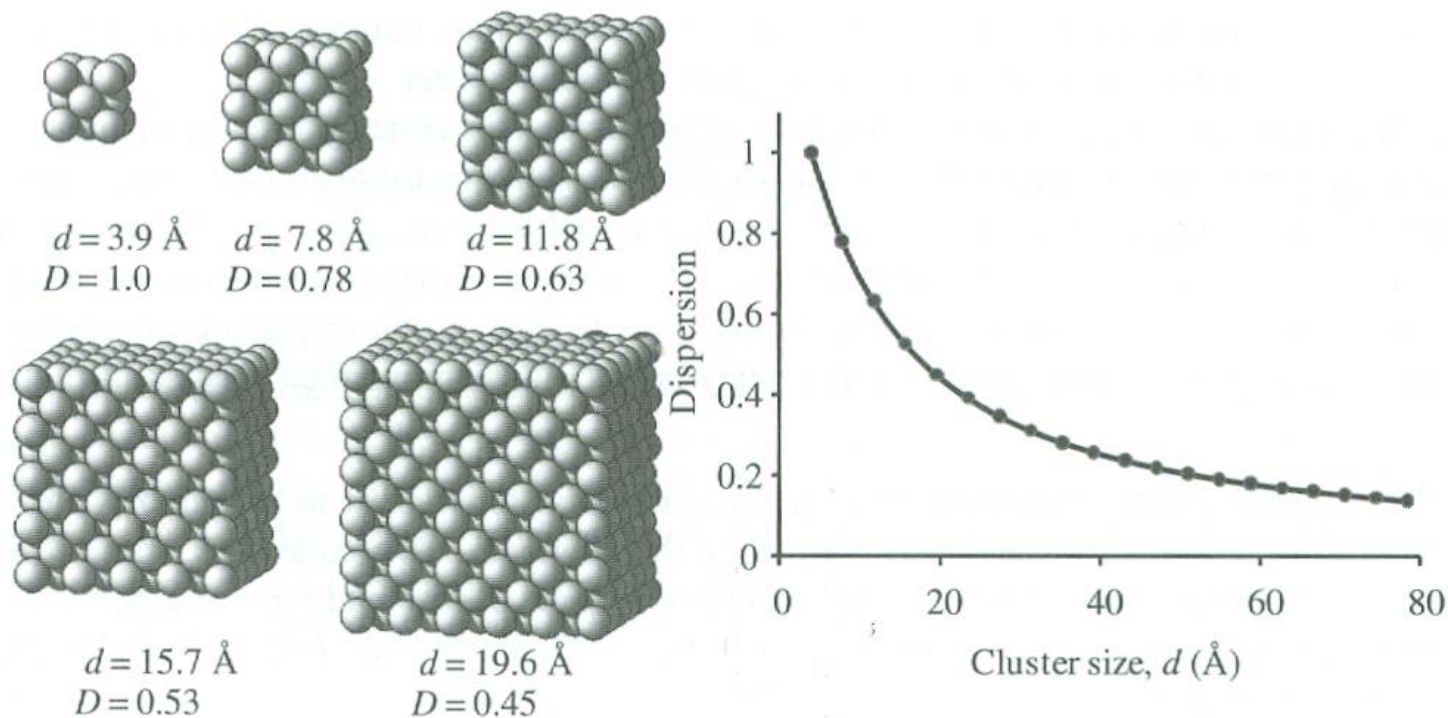


Figure 1.7. Cubic clusters with the face-centered cubic (fcc) packing of 14, 50, 110, 194, and 302 atoms (the left panel). In the smallest cluster, all of the atoms are on the surface. However, the dispersion defined as the number of surface atoms divided by the total number of atoms in the cluster, declines rapidly with increasing cluster size, which is shown in the right panel of the figure. The size d is the length of the edge of the cubic clusters. The lattice constant of the fcc clusters is assumed to be 3.9 Å, which is close to that of the Pt crystal.

- D depends somewhat on the shape of the particle and how the atoms are packed: the spherical cluster has smaller surface area than the cube cluster → lower dispersion (D) in round shape
- Higher D in catalysts → lower the material cost

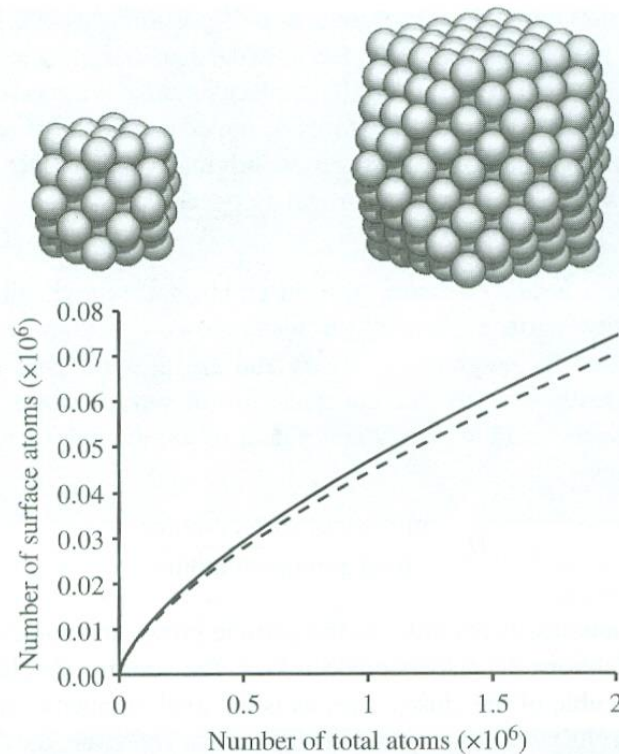


Figure 1.8. Truncated cubic clusters with the fcc packing of 55 and 309 atoms (the upper panel). The lower panel shows the number of surface atoms as a function of the total number of atoms for the cubic cluster (the solid line) and the truncated cubic cluster (the dashed line). Compared to the cubic cluster, the truncated cubic cluster is relatively rounder, so it has fewer atoms on the surface.

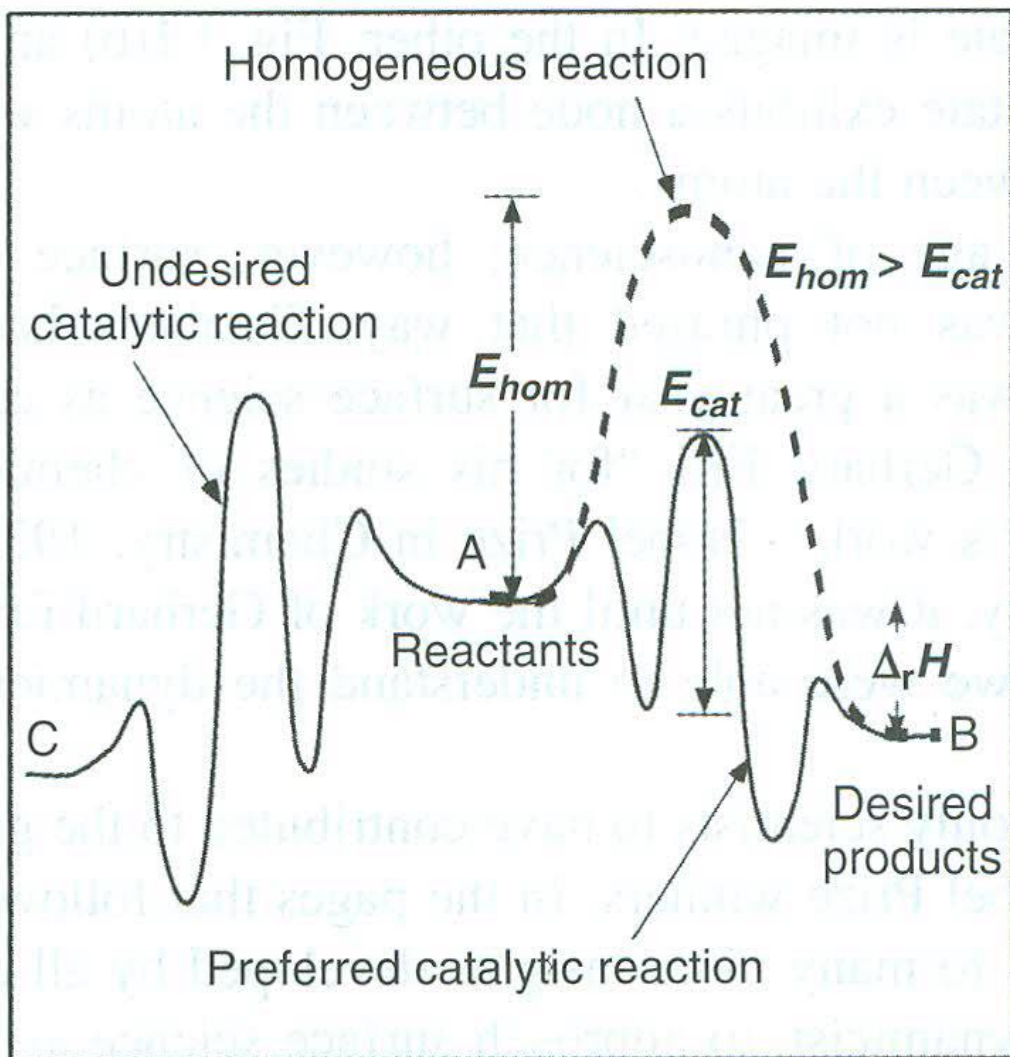
- Thin films: of great importance to many real-world problems and surface science

Internal surfaces: microporous solids

- Clays, graphite: layers → intercalation (for battery, filter, absorbent etc)
- Zeolites: ordered cages of molecular dimensions → large surface area

Surface science & heterogeneous catalysis

- The basis of chemical industry



Surface and Adsorbate Structure

1. Structural properties of solids and their surfaces
2. Electronic properties of solids and their surfaces
3. Vibrational properties of solids and their surfaces

Reading: Kolasinski, ch.1

Clean surfaces

- Ultra-high vacuum (UHV) conditions → atomically clean surfaces

the Flux, F , of molecules striking the surface of unit area at pressure P

$$F = \frac{N_A P}{\sqrt{2\pi MRT}} \quad (1.2) \quad \text{Z in (1.0.1)}$$

or

$$F \text{ (atoms}^{-1} \text{ cm}^{-2} \text{ s}^{-1}) = 2.63 \times 10^{20} \frac{P \text{ (Pa)}}{\sqrt{M \text{ (g mol}^{-1})T \text{ (K)}}} \quad (1.3)$$

or

$$F \text{ (atoms cm}^{-2} \text{ s}^{-1}) = 3.51 \times 10^{22} \frac{P \text{ (Torr)}}{\sqrt{M \text{ (g mol}^{-1})T \text{ (K)}}} \quad (1.4)$$

- UHV ($<1.33 \times 10^{-7} \text{ Pa} = 10^{-9} \text{ Torr}$) → to maintain a clean surface for ~ 1h

Fundamental Constants

Constant	Symbol	Value
Speed of light	c	2.998×10^{10} cm/sec = 2.998×10^8 m/sec
Planck's constant	h	6.626×10^{-27} erg · sec = 6.626×10^{-34} J · sec
Avogadro's number	N_A	6.022×10^{23} molecules/mole
Electron charge	e	1.602×10^{-21} coulombs = 4.803×10^{-10} esu
Gas constant	R	1.987 cal/deg/mole = 8.315 J/deg/mole
Boltzmann's constant	k_B	1.381×10^{-16} erg/deg = 1.381×10^{-23} J/deg = R/N_A
Gravitational constant	g	9.807 m/sec ²
Permittivity of vacuum	ϵ_0	8.854×10^{-12} C ² /J/m

Other Conversion Factors

1 atm	=	1.013×10^5 kg/m/sec ²
	=	1.013×10^5 N/m ²
	=	1.013×10^5 Pa
1 torr	=	133.3 N/m ²
1 debye	=	3.336×10^{-30} C · m

Energy Conversion Table^a

	erg	joule	cal	eV	cm ⁻¹
1 erg	1	10^{-7}	2.389×10^{-8}	6.242×10^{11}	5.034×10^{15}
1 joule	10^7	1	0.2389	6.242×10^{18}	5.034×10^{22}
1 cal	4.184×10^7	4.184	1	2.612×10^{19}	2.106×10^{23}
1 eV	1.602×10^{-12}	1.602×10^{-19}	3.829×10^{-20}	1	8066.0
1 cm ⁻¹	1.986×10^{-16}	1.986×10^{-23}	4.747×10^{-24}	1.240×10^{-4}	1

^aFor example, 1 erg = 2.389×10^{-8} cal.

cf.

- Adsorption → always an exothermic process → positive heat of adsorption, ΔH_{ads}

the residence time, τ , of an adsorbed atom

$$\tau = \tau_0 \exp\left(\frac{\Delta H_{\text{ads}}}{RT}\right) \quad (1.5)$$

where τ_0 is correlated with the surface atom vibration times ($\sim 10^{-12}$ s), R gas constant, T temperature. τ can be 1s or longer at 300K for $\Delta H_{\text{ads}} > 63$ kJ/mol

the surface concentration σ (in molecules cm^{-2}) of adsorbed molecules on an initially clean surface → product of the incident flux (F) and the residence time

$$\sigma = F\tau$$

substrate-adsorbate bonds are usually stronger than bonds between adsorbed molecules

Surface structure

1st layer of close-packed spheres

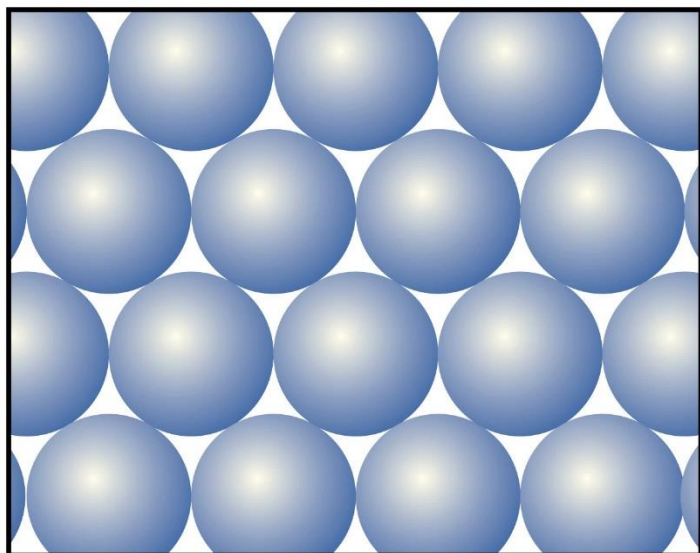


Figure 20-32
Atkins Physical Chemistry, Eighth Edition
© 2006 Peter Atkins and Julio de Paula

2nd layer of close-packed spheres

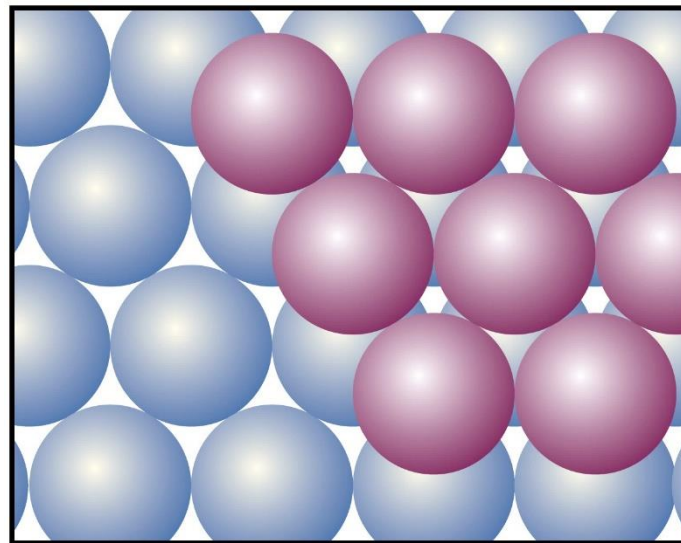


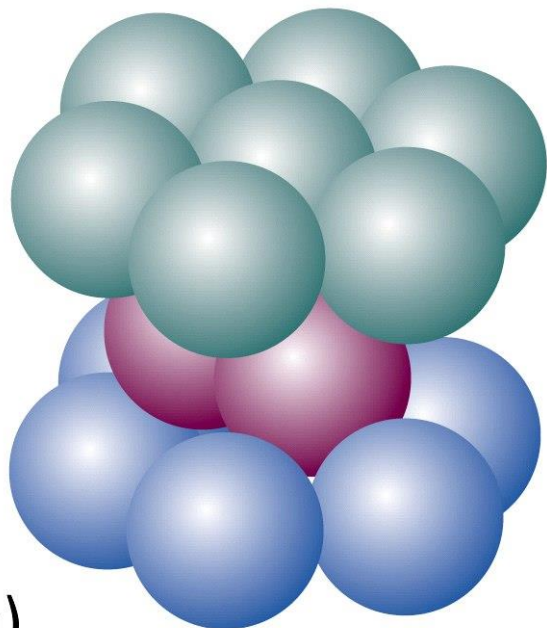
Figure 20-33
Atkins Physical Chemistry, Eighth Edition
© 2006 Peter Atkins and Julio de Paula

3rd layer of close-packed spheres: ABA (hexagonal close-packed)
CBA (cubic close-packed)

hcp: ABABAB...

ccp: ABCABC...

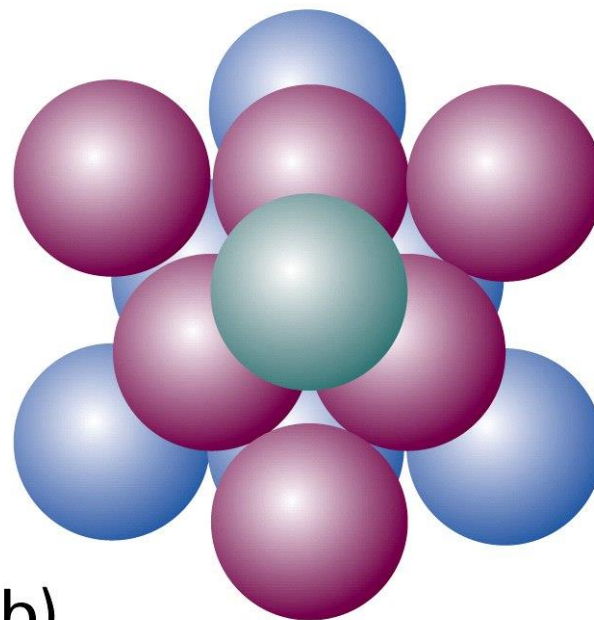
hcp



(a)

Figure 20-35
Atkins Physical Chemistry, Eighth Edition
© 2006 Peter Atkins and Julio de Paula

fcc (one example of ccp)



(b)

fcc (face-centered cubic)

close-packed spheres (hcp, ccp)

coordination numbers = 12

packing fraction: 0.740 (26% empty space)

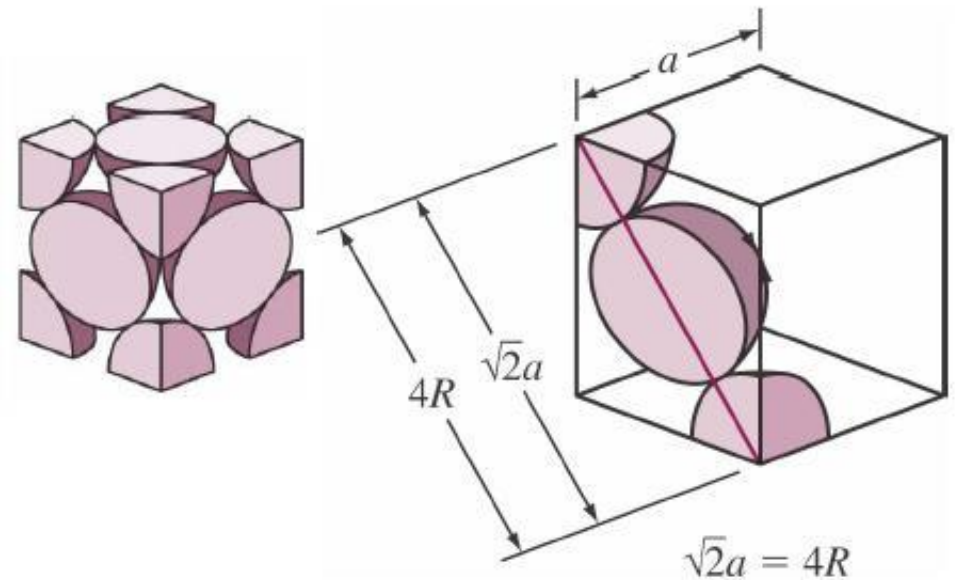
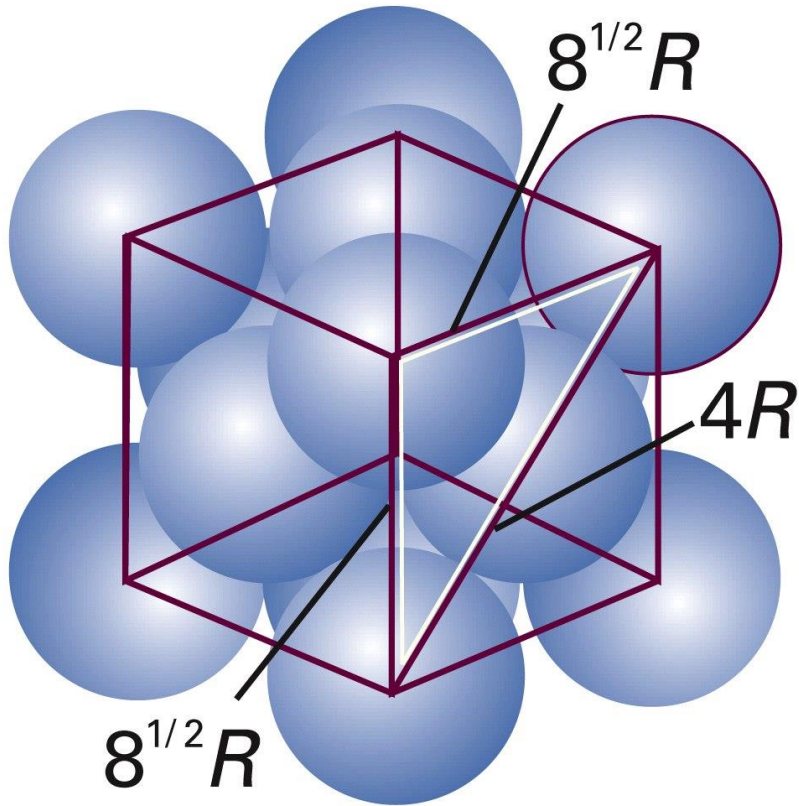


Figure 20-36
Atkins Physical Chemistry, Eighth Edition
© 2006 Peter Atkins and Julio de Paula

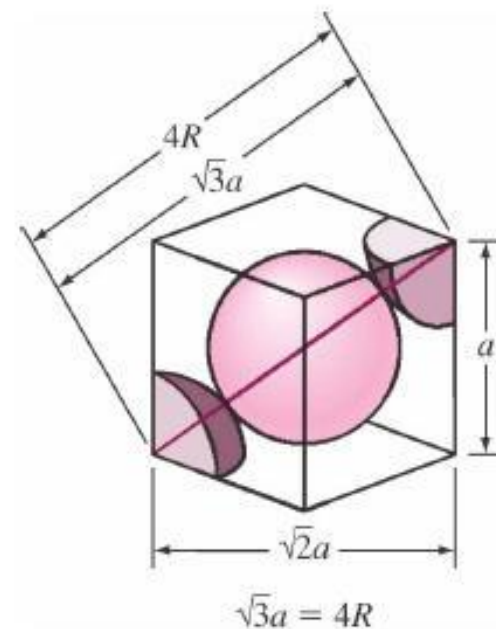
Table 20.2 The crystal structures of some elements

Structure	Element
hcp*	Be, Cd, Co, He, Mg, Sc, Ti, Zn Ru
fcc* (ccp, cubic F)	Ag, Al, Ar, Au, Ca, Cu, Kr, Ne, Ni, Pd, Pb, Pt, Rh, Rn, Sr, Xe
bcc (cubic I)	Ba, Cs, Cr, Fe, K, Li, Mn, Mo, Rb, Na, Ta, W, V
cubic P	Po

* Close-packed structures.

Table 20-2
Atkins Physical Chemistry, Eighth Edition
 © 2006 Peter Atkins and Julio de Paula

bcc (body-centered cubic)
 coordination numbers = 8
 packing fraction: 0.680 (32% empty space)



Miller index: crystal planes

plane (hkl) : reciprocals of intersection distances, set $\{001\} = (100), (010), (001)$

Direction $[hkl]$: direction normal to a plane (hkl)

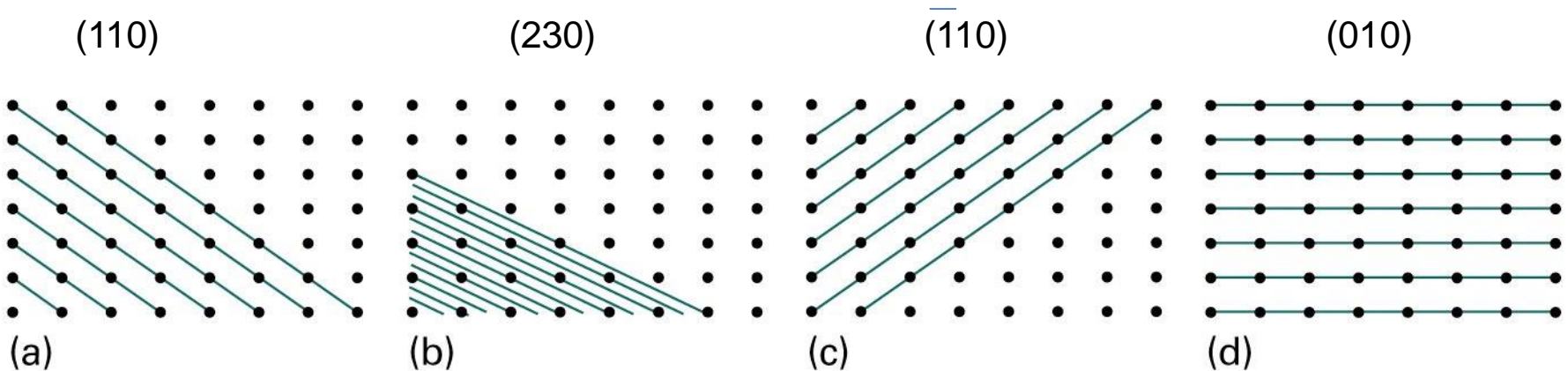
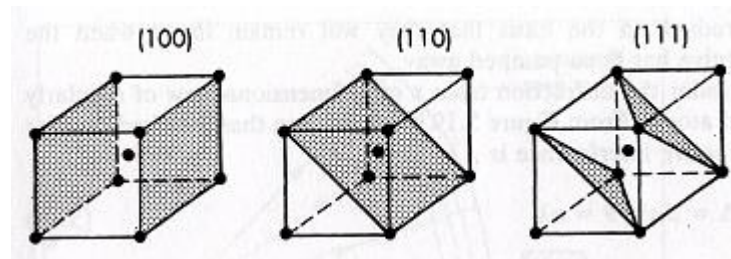


Figure 20-9
Atkins Physical Chemistry, Eighth Edition
© 2006 Peter Atkins and Julio de Paula



fcc

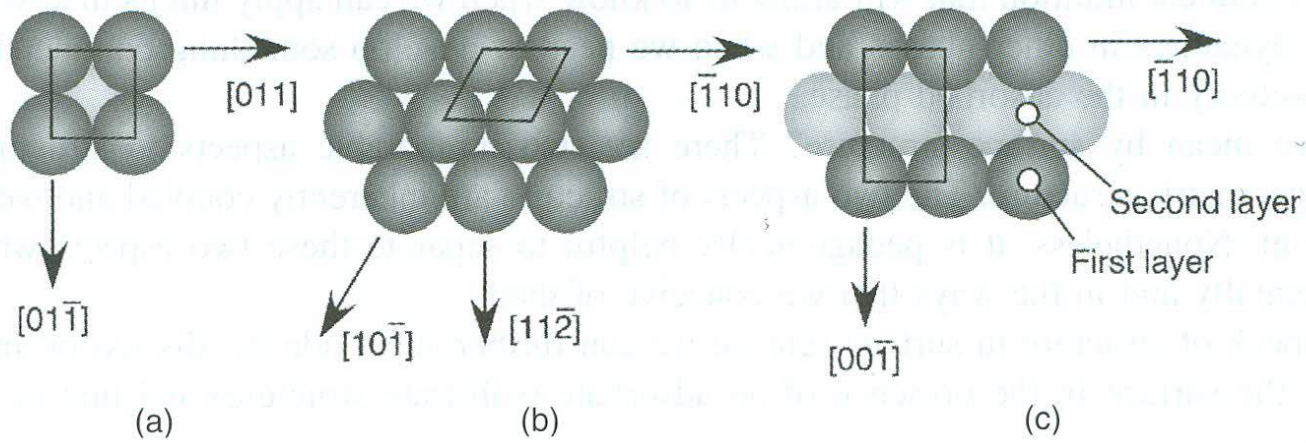
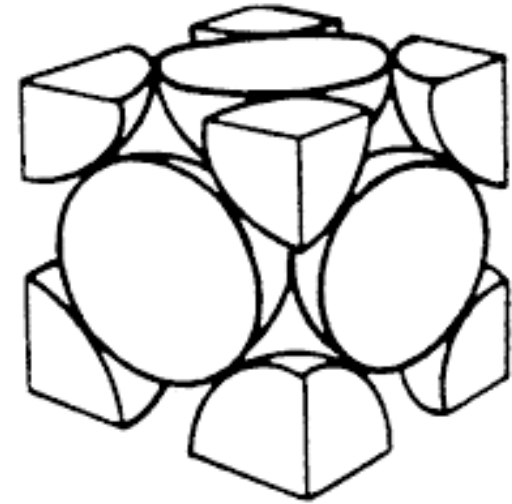
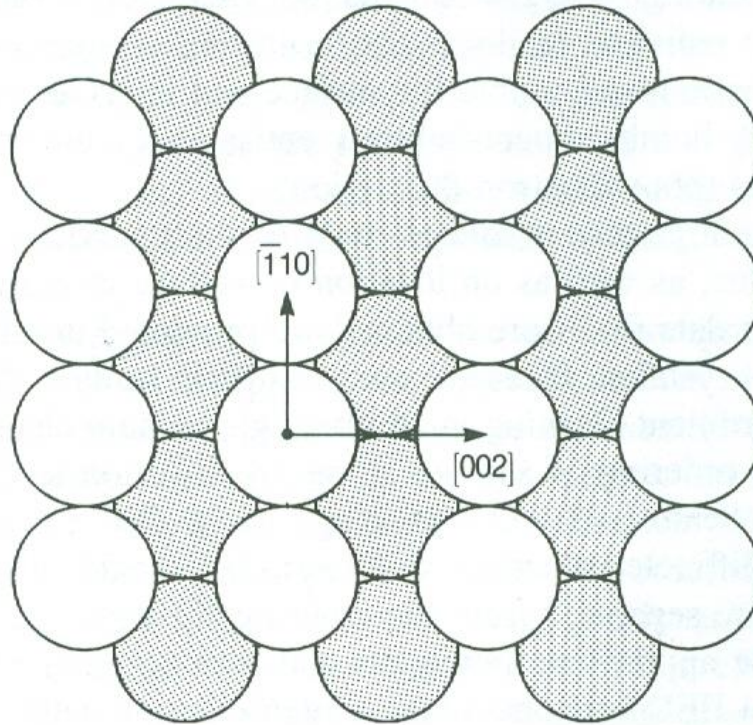
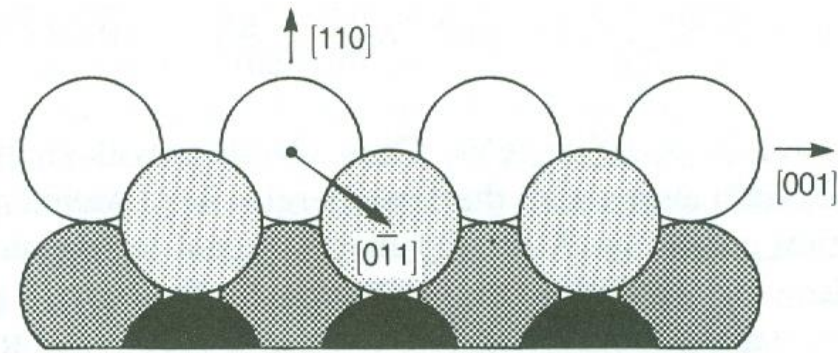


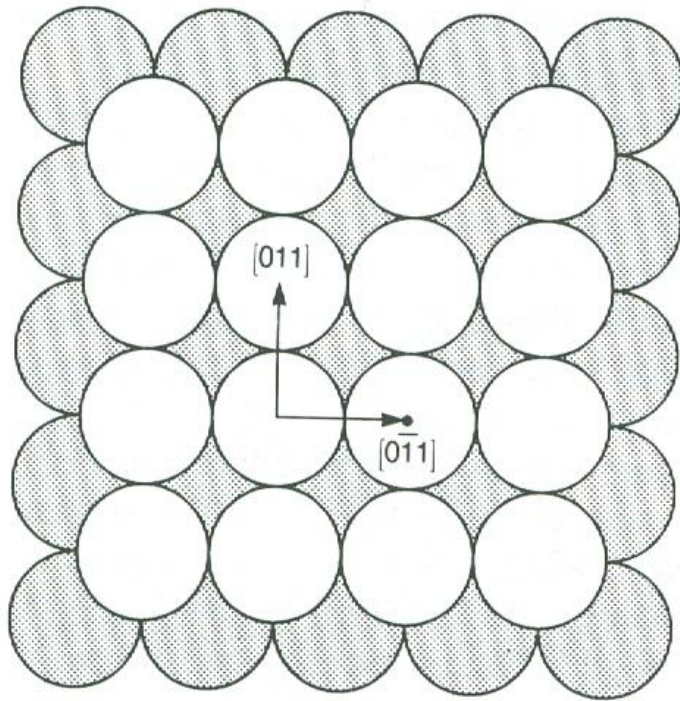
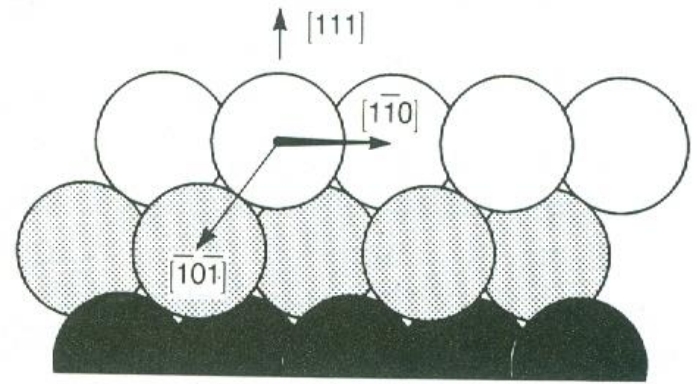
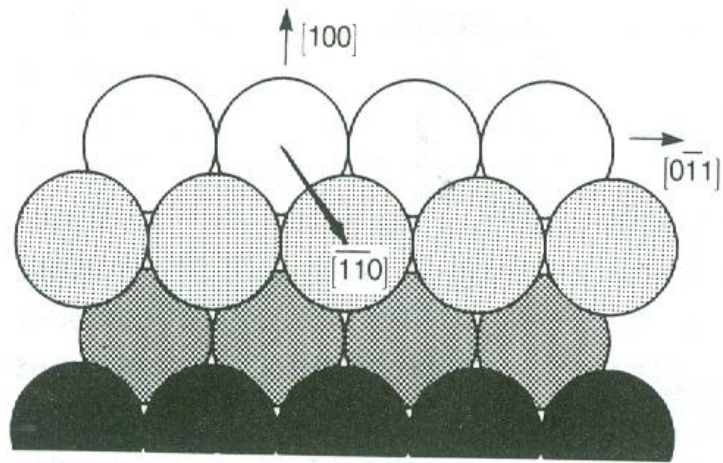
Figure 1.1 Hard sphere representations of face-centred cubic (fcc) low index planes: (a) $fcc(100)$; (b) $fcc(111)$; (c) $fcc(110)$.



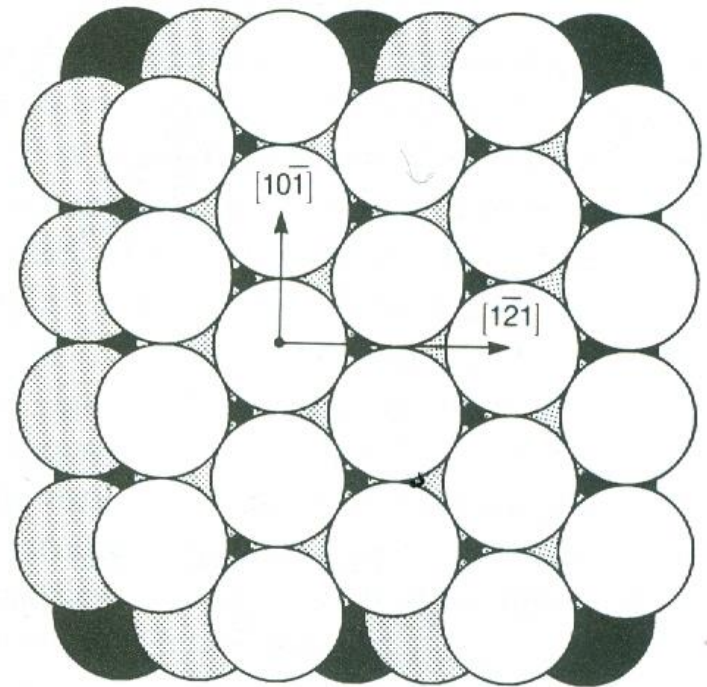
fcc (110)

(a)

Figure 2.8. Top views and side views of the face-centered cubic (fcc) crystal surfaces: (a) (110), (b) (100), and (c) (111)



fcc (100)
(b)



fcc (111)
(c)

Figure 2.8. (Continued)

- Ideal structure of low-Miller-index surfaces of face-centered cubic (fcc)

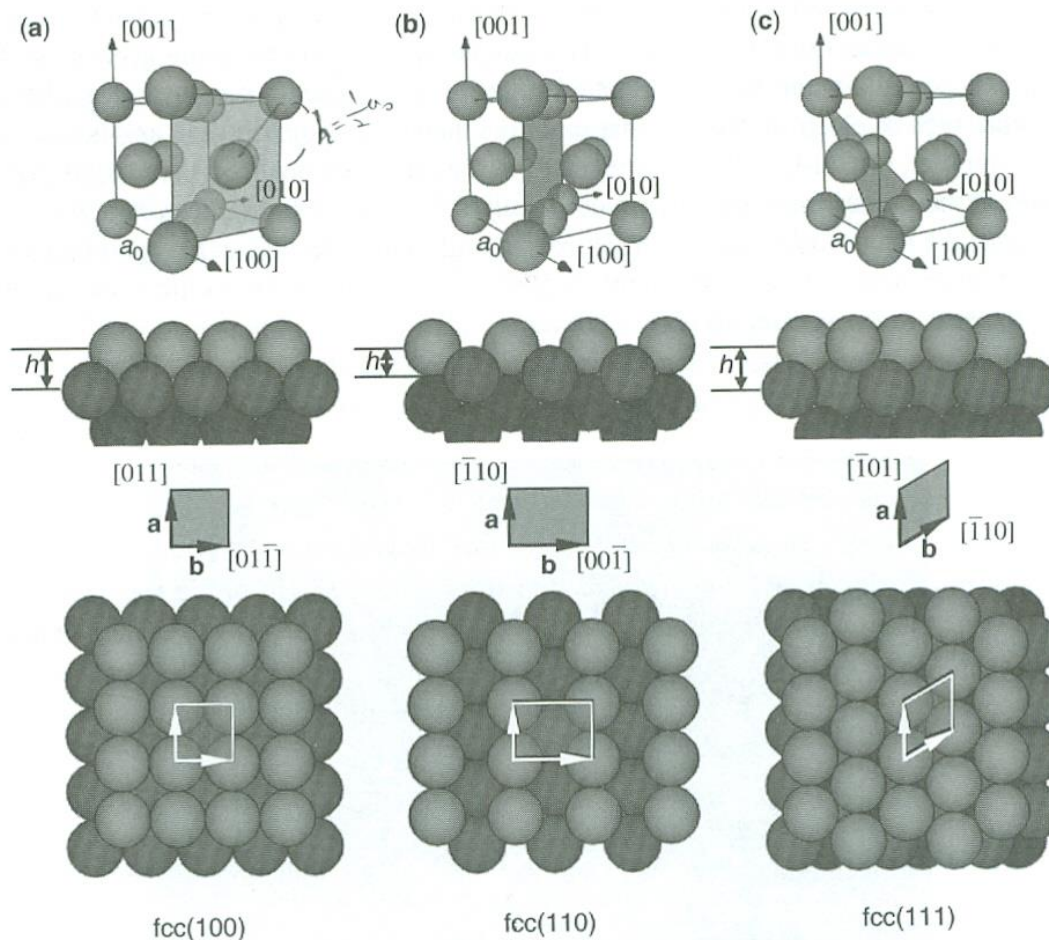


Figure 2.8. Unreconstructed surfaces of the fcc crystal surfaces, where a_0 is the lattice constant of the crystal, \mathbf{a} and \mathbf{b} are the unit-cell vectors, and h is the distance between the first and the second layer. (a) fcc(100): $|\mathbf{a}| = |\mathbf{b}| = (\sqrt{2}/2)a_0$, and $h = \frac{1}{2}a_0$. To obtain the second layer, shift the first layer by $\frac{1}{2}\mathbf{a} + \frac{1}{2}\mathbf{b}$ in the plane, then $\frac{1}{2}a_0$ in the $[\bar{1}00]$ direction. (b) fcc(110): $|\mathbf{a}| = (\sqrt{2}/2)a_0$, $|\mathbf{b}| = a_0$, and $h = (\sqrt{2}/4)a_0$. To obtain the second layer, shift the first layer by $\frac{1}{2}\mathbf{a} + \frac{1}{2}\mathbf{b}$ in the plane, then $(\sqrt{2}/4)a_0$ in the $[\bar{1}\bar{1}0]$ direction. (c) fcc(111): $|\mathbf{a}| = |\mathbf{b}| = (\sqrt{2}/2)a_0$, and $h = (\sqrt{3}/3)a_0$. To obtain the second layer, shift the first layer by $\frac{1}{3}\mathbf{a} + \frac{1}{3}\mathbf{b}$ in the plane, then $(\sqrt{3}/3)a_0$ in the $[\bar{1}\bar{1}\bar{1}]$ direction. (See color insert.)

bcc

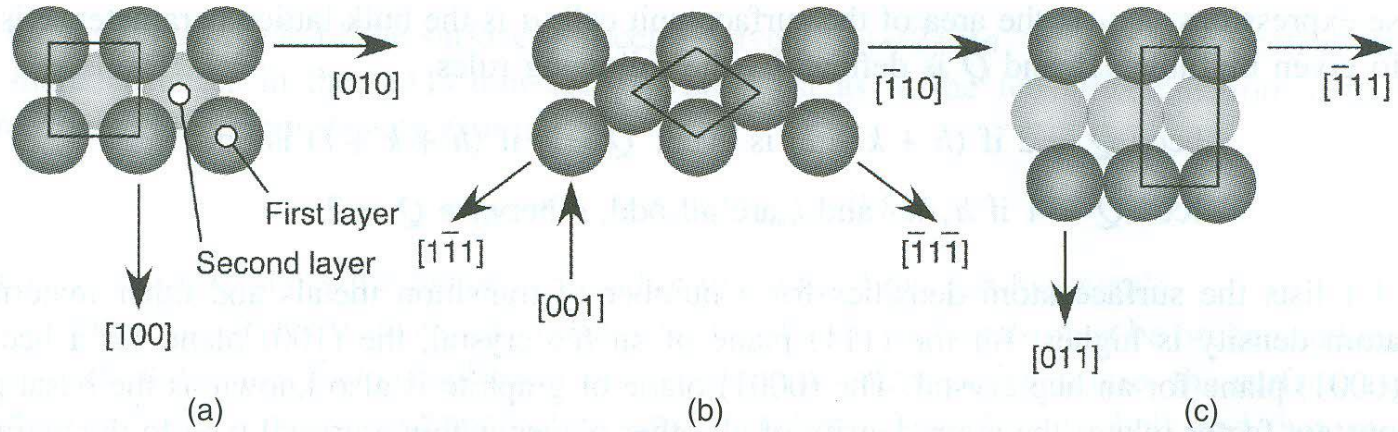


Figure 1.2 Hard sphere representations of body-centred cubic (bcc) low index planes: (a) $bcc(100)$; (b) $bcc(110)$; (c) $bcc(211)$.

hcp

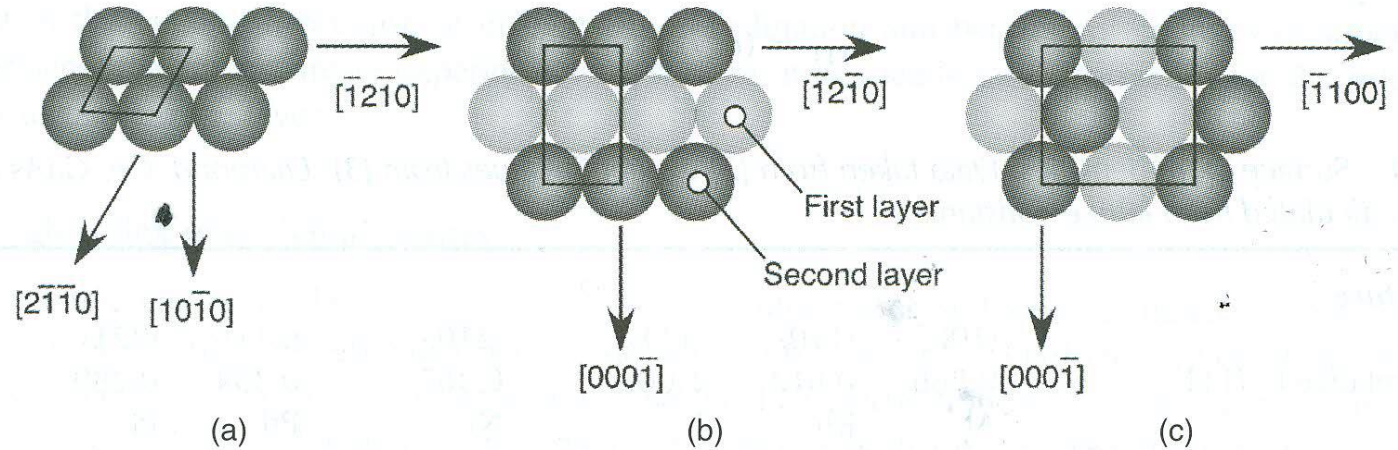
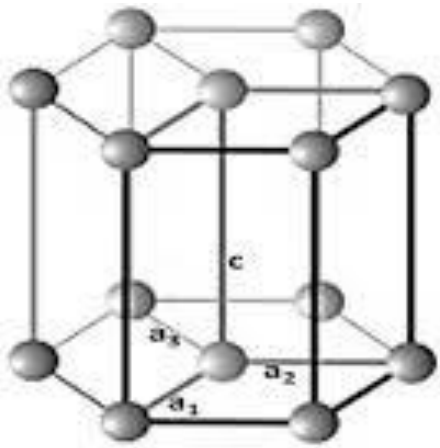
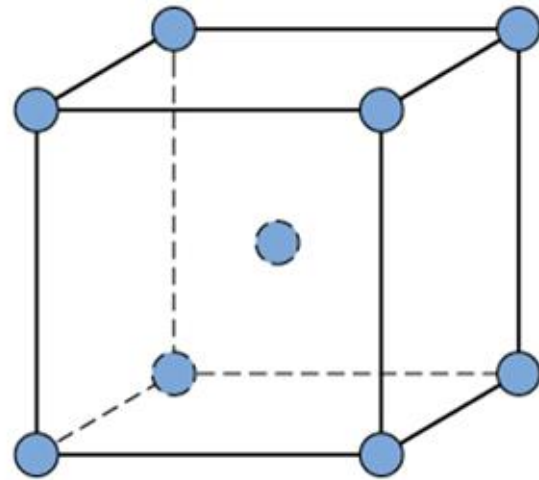
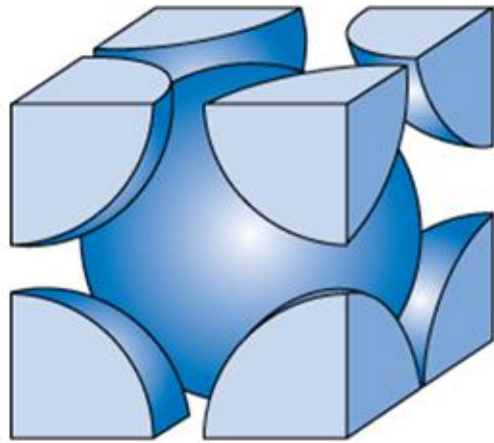
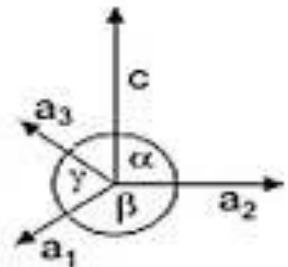


Figure 1.3 Hard sphere representations of hexagonal close-packed (hcp) low index planes: (a) $hcp(001) = (0001)$; (b) $hcp(10\bar{1}0) = hcp(100)$; (c) $hcp(11\bar{2}0) = hcp(110)$.



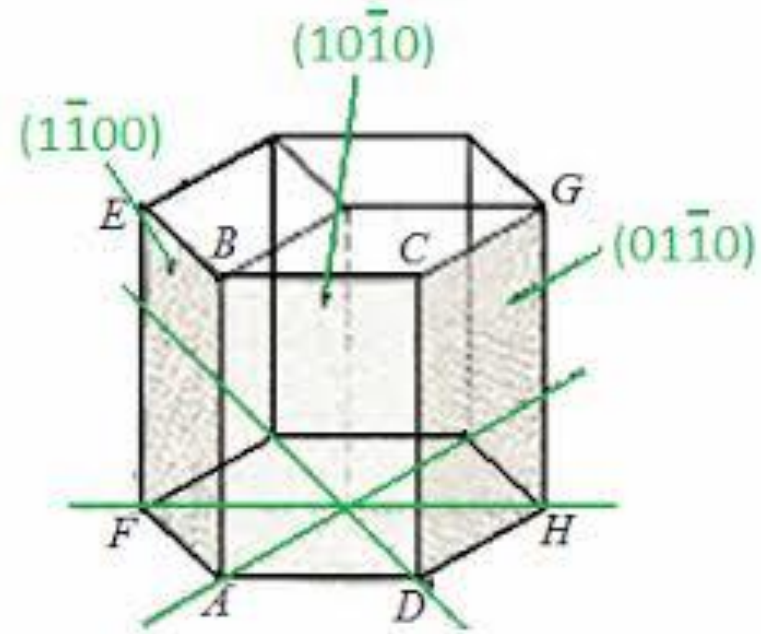
(a)

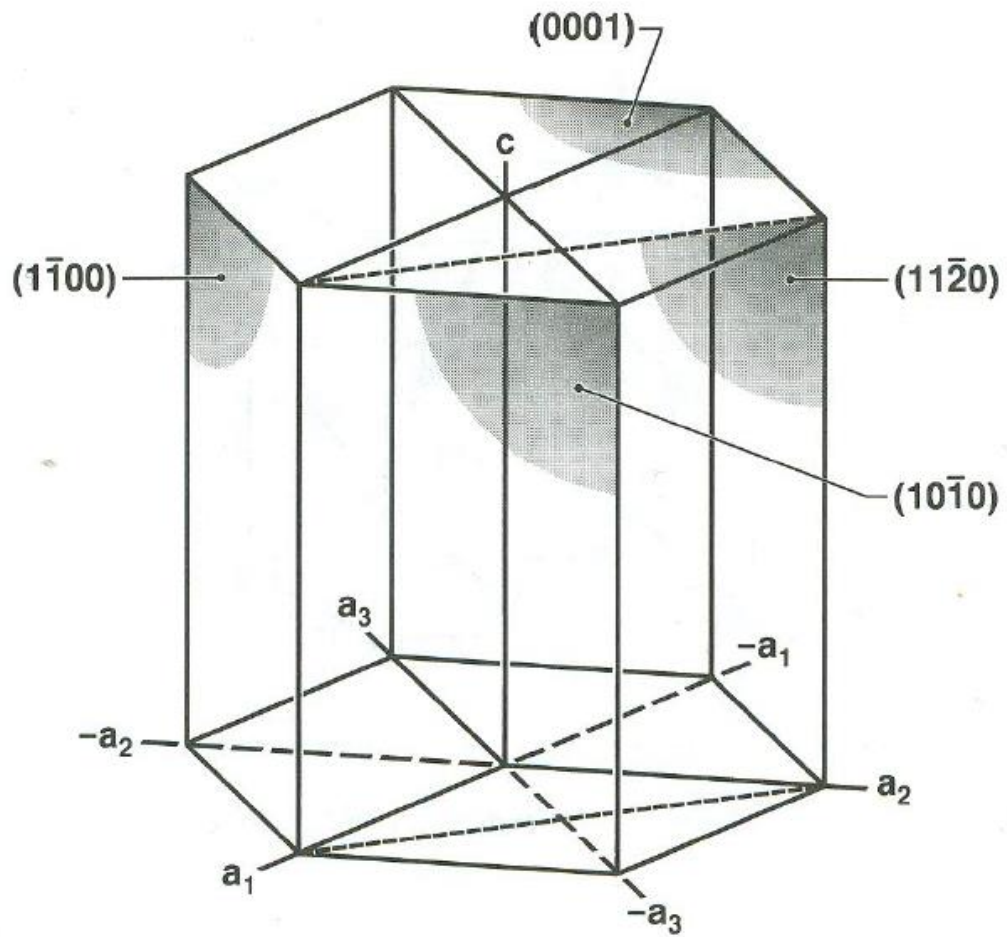


(b)

$$a_1 = a_2 = a_3 \neq c$$

$$\alpha = \gamma = 90^\circ \quad \beta = 120^\circ$$





- Ideal structure of low-Miller-index surfaces of body-centered cubic (bcc)

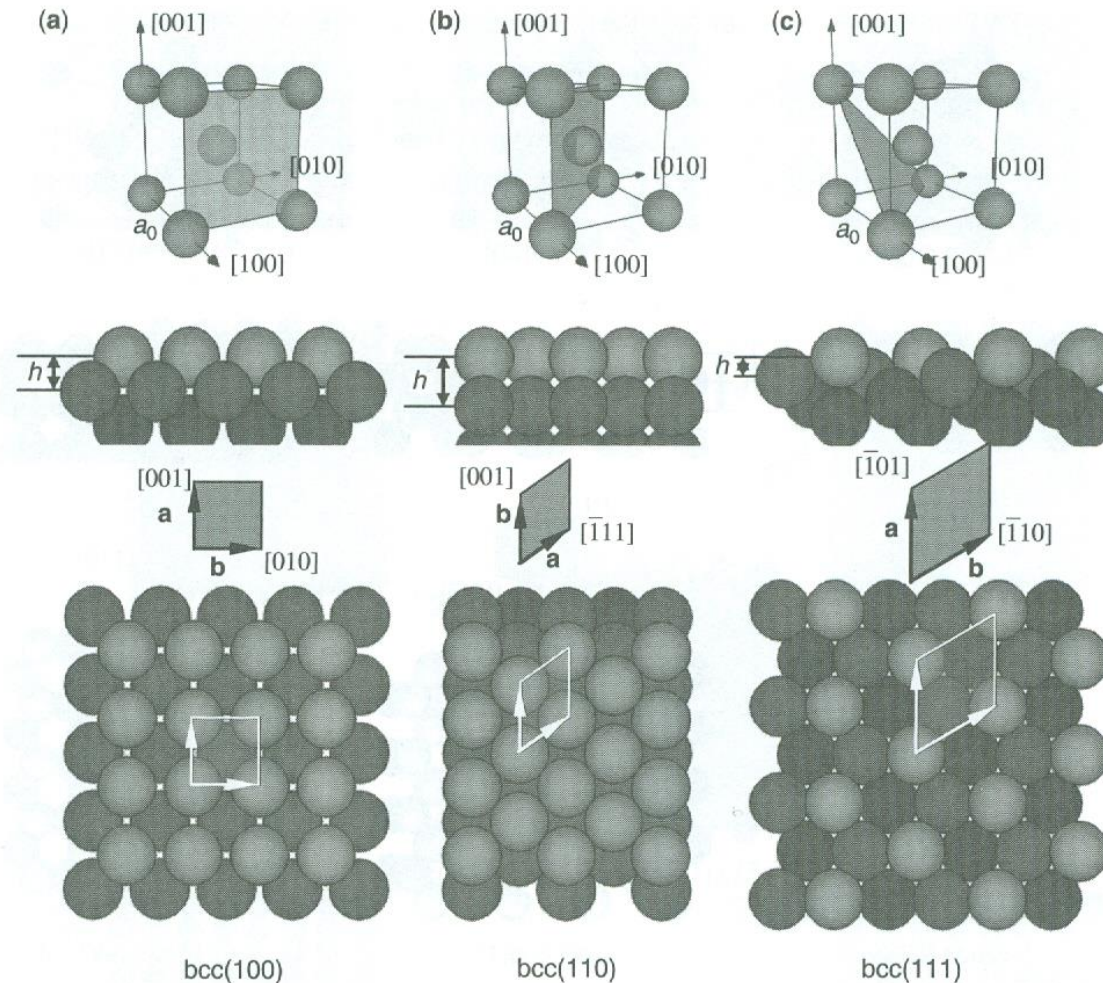


Figure 2.9. Unreconstructed surfaces of the bcc crystal surfaces, where a_0 is the lattice constant of the crystal, \mathbf{a} and \mathbf{b} are the unit-cell vectors, h is the distance between the first and the second layer. (a) bcc(100): $|\mathbf{a}| = |\mathbf{b}| = a_0$, and $h = \frac{1}{2}a_0$. To obtain the second layer, shift the first layer by $\frac{1}{2}\mathbf{a} + \frac{1}{2}\mathbf{b}$ in the plane, then $\frac{1}{2}a_0$ in the $[\bar{1}00]$ direction. (b) bcc(110): $|\mathbf{a}| = (\sqrt{3}/2)a_0$, $|\mathbf{b}| = a_0$, and $h = (\sqrt{2}/2)a_0$. To obtain the second layer, shift the first layer by $\frac{1}{2}\mathbf{b}$ in the plane, then $\frac{1}{2}a_0$ in the $[\bar{1}\bar{1}0]$ direction. (c) bcc(111): $|\mathbf{a}| = |\mathbf{b}| = \sqrt{2}a_0$, and $h = (\sqrt{3}/6)a_0$. To obtain the second layer, shift the first layer by $\frac{1}{3}\mathbf{a} + \frac{1}{3}\mathbf{b}$ in the plane, then $(\sqrt{3}/6)a_0$ in the $[\bar{1}\bar{1}\bar{1}]$ direction. (See color insert.)

- Ideal structure of low-Miller-index surfaces of diamond cubic crystals

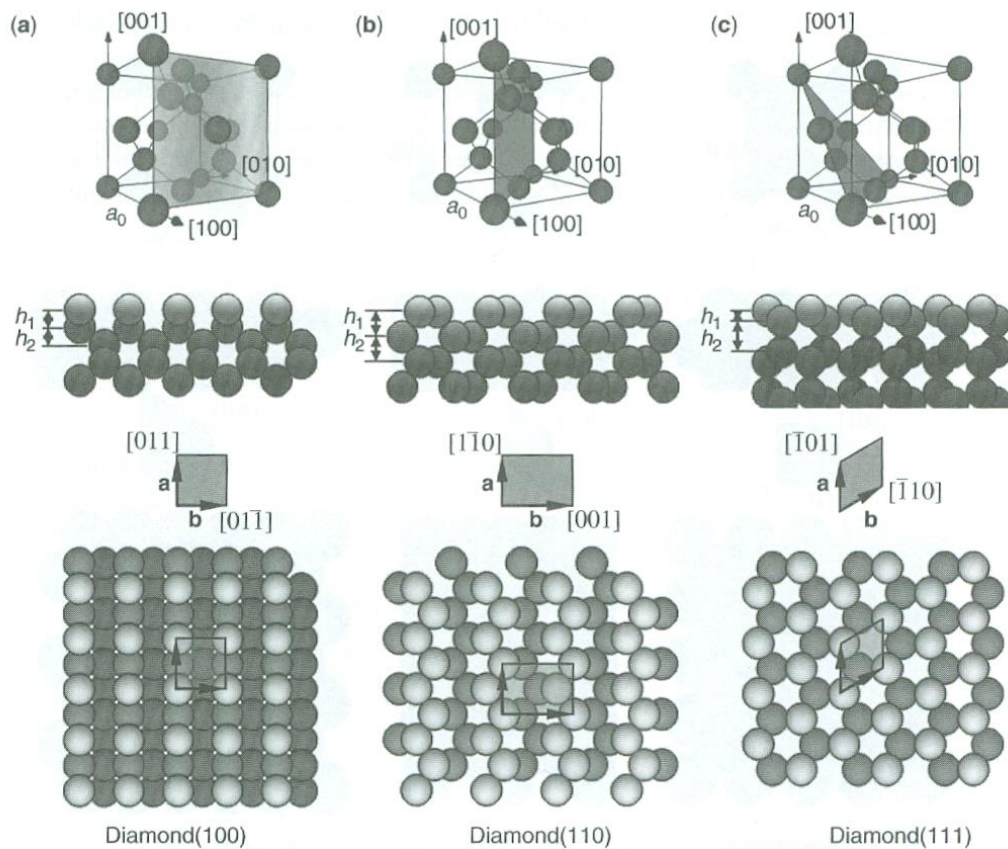


Figure 2.10. Unreconstructed surfaces of the diamond crystal surfaces, where a_0 is the lattice constant of the crystal, \mathbf{a} and \mathbf{b} are the unit-cell vectors, h_1 and h_2 are the distances between the first and the second layer, and the second and the third layer, respectively. (a) Diamond(100): $|\mathbf{a}| = |\mathbf{b}| = (\sqrt{2}/2)a_0$, and $h_1 = h_2 = \frac{1}{4}a_0$. To obtain the second layer, shift the first layer by $\frac{1}{2}\mathbf{a}$ in the plane, then $\frac{1}{4}a_0$ in the $[\bar{1}00]$ direction. To obtain the third layer, shift the first layer by $\frac{1}{2}\mathbf{a} + \frac{1}{2}\mathbf{b}$ in the plane, then $\frac{1}{2}a_0$ in the $[\bar{1}00]$ direction. (b) Diamond(110): $|\mathbf{a}| = (\sqrt{2}/2)a_0$, $|\mathbf{b}| = a_0$, and $h_1 = h_2 = (\sqrt{2}/2)a_0$. To obtain the second layer, shift the first layer by $\frac{1}{2}\mathbf{a} + \frac{1}{2}\mathbf{b}$ in the plane, then $(\sqrt{2}/2)a_0$ in the $[\bar{1}\bar{1}0]$ direction. To obtain the third layer, shift the first layer by $\sqrt{2}a_0$ in the $[\bar{1}\bar{1}0]$ direction. (c) Diamond(111): $|\mathbf{a}| = |\mathbf{b}| = (\sqrt{2}/2)a_0$, $h_1 = (\sqrt{3}/12)a_0$, and $h_2 = (\sqrt{3}/4)a_0$. To obtain the second layer, shift the first layer by $\frac{1}{3}\mathbf{a} + \frac{1}{3}\mathbf{b}$ in the plane, then $(\sqrt{3}/12)a_0$ in the $[\bar{1}\bar{1}\bar{1}]$ direction. To obtain the second layer, shift the first layer by $\frac{1}{3}\mathbf{a} + \frac{1}{3}\mathbf{b}$ in the plane, then $(\sqrt{3}/3)a_0$ in the $[\bar{1}\bar{1}\bar{1}]$ direction. (See color insert.)

d_{hkl}

Separation of planes

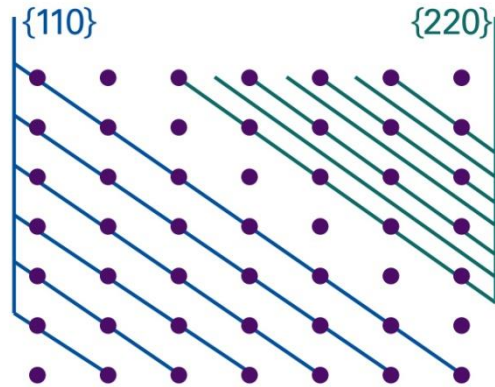
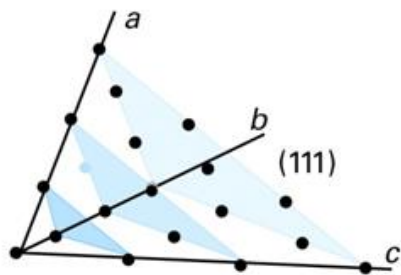
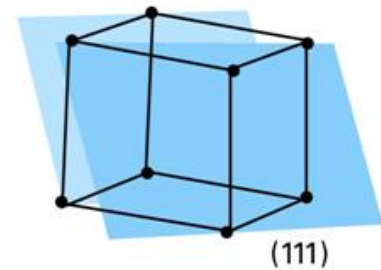
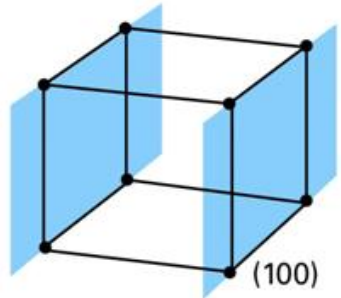
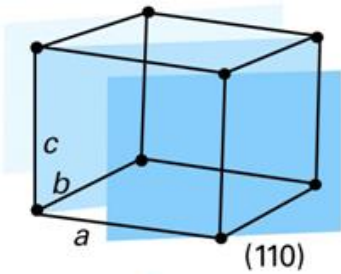
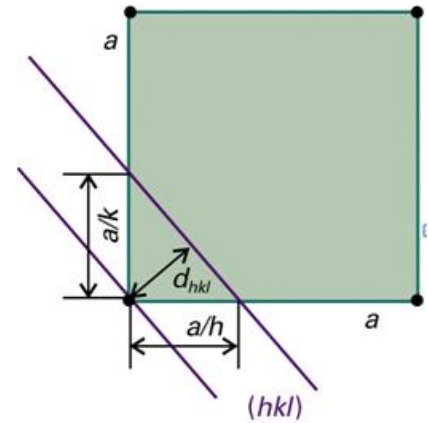


Figure 20-12
Atkins Physical Chemistry, Eighth Edition
© 2005 Peter Atkins and Julio de Paula



$$\frac{1}{d_{hkl}^2} = \frac{h^2 + k^2 + l^2}{a^2} \quad \text{or} \quad d_{hkl} = \frac{a}{(h^2 + k^2 + l^2)^{1/2}} \quad ; \text{cubic}$$

$$\frac{1}{d_{hkl}^2} = \frac{h^2}{a^2} + \frac{k^2}{b^2} + \frac{l^2}{c^2} \quad ; \text{orthorhombic}$$

Surface atom density (σ_0)

Table 1.1 Surface atom densities. Data taken from [2] except Si values from [3]. Diamond, Ge, GaAs and graphite calculated from lattice constants

fcc structure

Plane	(100)	(110)	(111)	(210)	(211)	(221)	
Density relative to (111)	0.866	0.612	1.000	0.387	0.354	0.289	
Metal	Al	Rh	Ir	Ni	Pd	Pt	Cu
Density of (111)/cm ⁻² × 10 ⁻¹⁵	1.415	1.599	1.574	1.864	1.534	1.503	1.772
Metal	Ag	Au					
Density of (111)/cm ⁻² × 10 ⁻¹⁵	1.387	1.394					

bcc structure

Plane	(100)	(110)	(111)	(210)	(211)	(221)	
Density relative to (110)	0.707	1.000	0.409	0.316	0.578	0.236	
Metal	V	Nb	Ta	Cr	Mo	W	Fe
Density of (100)/cm ⁻² × 10 ⁻¹⁵	1.547	1.303	1.299	1.693	1.434	1.416	1.729

hcp structure

Plane	(0001)	(10 $\bar{1}$ 0)	(10 $\bar{1}$ 1)	(10 $\bar{1}$ 2)	(11 $\bar{2}$ 2)	(11 $\bar{2}$ 2)	
Density relative to (0001)	1.000	$\frac{3}{2r}$	$\frac{\sqrt{3}}{(4r^3 + 3)^{1/2}}$	$\frac{\sqrt{3}}{(4r^3 + 12)^{1/2}}$	$\frac{1}{r}$	$\frac{1}{2(r^3 + 1)^{1/2}}$	
Metal	Zr	Hf	Re	Ru	Os	Co	Zn
Density of (0001)/cm ⁻² × 10 ⁻¹⁵	1.110	1.130	1.514	1.582	1.546	1.830	1.630
Axial ratio $r = c/a$	1.59	1.59	1.61	1.58	1.58	1.62	1.86
Metal	Cd						
Density of (0001)/cm ⁻² × 10 ⁻¹⁵	1.308						
Axial ratio $r = c/a$	1.89						

		Diamond lattice			Zincblende		Graphite
Element	C	Si	Ge		GaAs		C
Areal Density/cm ⁻² × 10 ⁻¹⁵							basal plane
(100)	1.57	0.6782	0.627		0.626		3.845
(111)	1.82	0.7839	0.724		0.723		

High index and vicinal planes

- Dislocation: mismatch of atomic planes

dislocation densities: $\sim 10^6$ - 10^8 cm^{-2} at metal or ionic crystal surfaces, 10^4 - 10^6 cm^{-2} in semiconductor or insulator crystals

surface concentration of atoms $\sim 10^{15}$ cm^{-2} \rightarrow each terrace contains roughly $10^{15}/10^6 = 10^9$ atoms

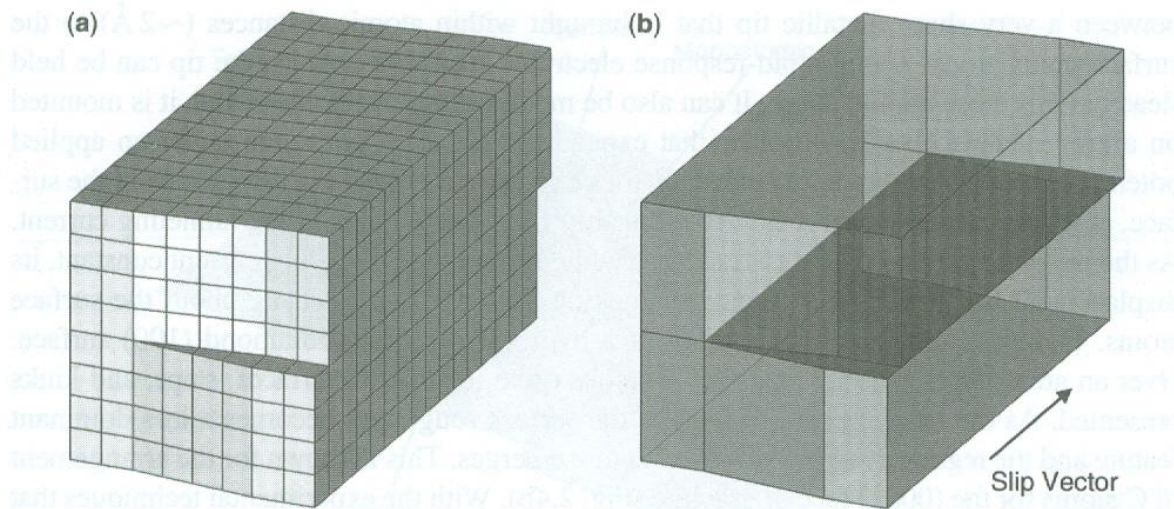


Figure 2.2. One type of screw dislocation giving rise to (a) atomic steps at the surface and (b) the slip plane that produces the dislocation (indicated by the dark plane) and, ultimately, the defects at the surface (steps and kinks).

- Model of surface structure of solids

Atoms in terraces are surrounded by the largest number of nearest neighbors. Atoms in steps have fewer neighbors, and atoms in kink sites have even fewer. Or line defects (steps and kinks) and point defects (atomic vacancies and adatoms)

On a rough surface, 10~20% steps, 5% kink, <1% point defects

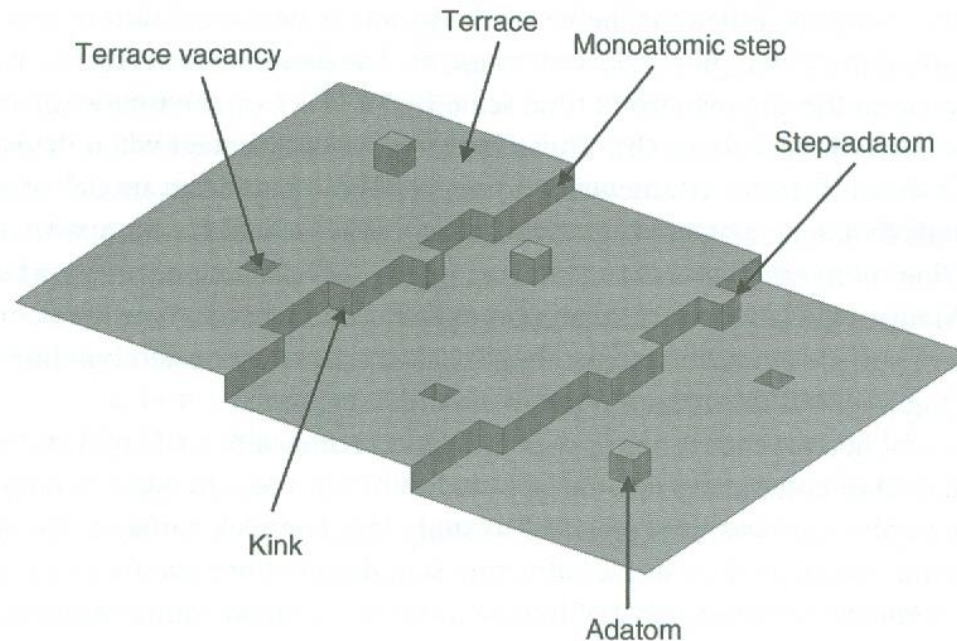


Figure 2.5. Model of a heterogeneous solid surface depicting different surface sites. These sites are distinguishable by their number of nearest neighbors.

- Notation of high-Miller-index, stepped surfaces

(755) Surface of fcc:

6 atoms wide (111) terrace,
1 atom height (100) step

Notation of terrace + step:

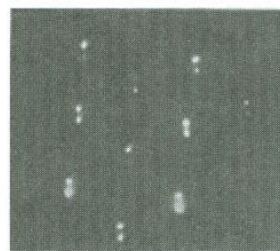
$W(hkl) \times (h_s k_s l_s)$

Kinked surface

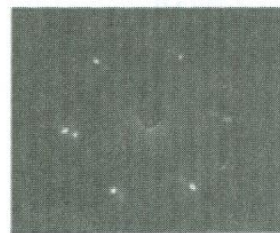
e.g., (10,8,7) =
7(111) \times (310)



Pt(111)



Pt(755)
Pt[6(111) \times (100)]



Pt(10,8,7)
Pt[7(111) \times (310)]

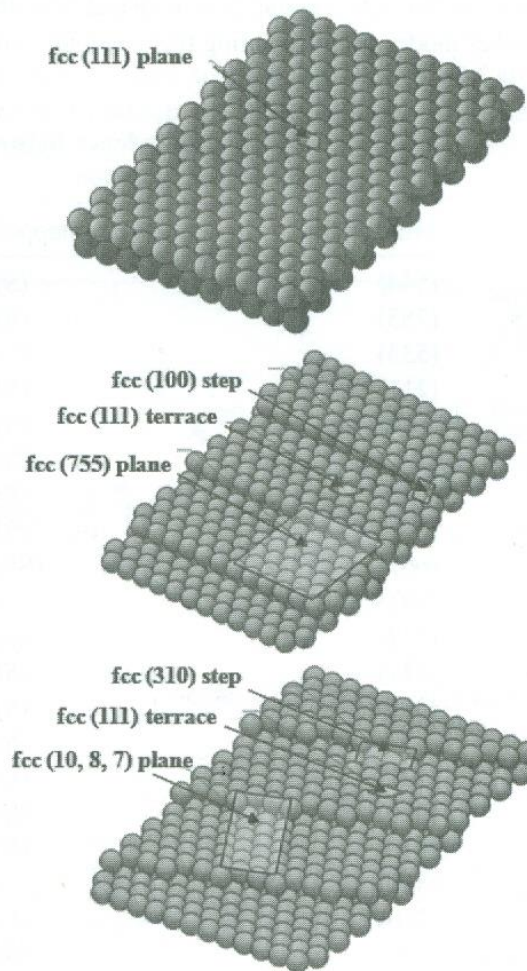


Figure 2.12. Surface structures in real space and LEED diffraction patterns of the flat Pt(111), stepped Pt(755), and kinked Pt(10,8,7) crystal faces.

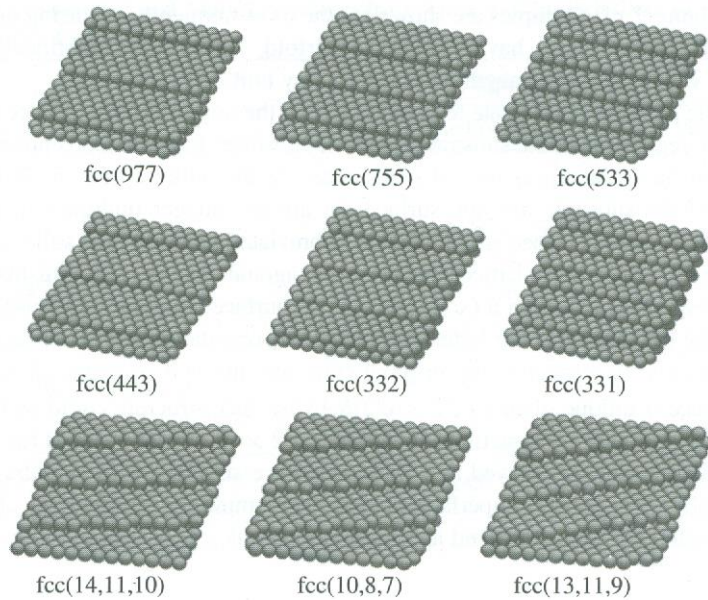


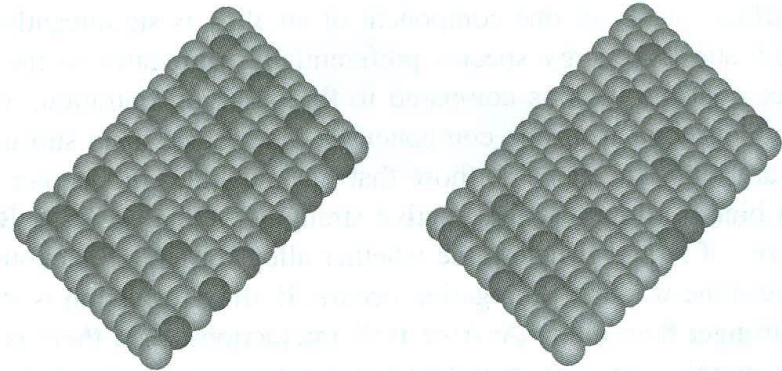
Figure 2.13. Schematic representation of the surface structures of several stepped (the first two rows) and kinked (the bottom row) crystal faces deduced from the bulk unit cell. Contraction of interlayer spacing and other modes of restructuring that are commonly observed are not shown.

TABLE 2.2 Correspondence between the Miller-Index and Stepped-Surface Notation

Miller Index	Stepped-Surface Designation
(544)	(S)-[9(111) × (100)]
(755)	(S)-[6(111) × (100)]
(533)	(S)-[4(111) × (100)]
(211)	(S)-[3(111) × (100)]
(311)	(S)-[2(111) × (100)]
	(S)-[2(100) × (111)]
(511)	(S)-[3(100) × (111)]
(711)	(S)-[4(100) × (111)]
(665)	(S)-[12(111) × (111)]
(997)	(S)-[9(111) × (111)]
(332)	(S)-[6(111) × (111)]
(221)	(S)-[4(111) × (111)]
(331)	(S)-[3(111) × (111)]
	(S)-[2(110) × (111)]
(771)	(S)-[4(110) × (111)]
(610)	(S)-[6(100) × (110)]
(410)	(S)-[4(100) × (110)]
(310)	(S)-[3(100) × (110)]
(210)	(S)-[2(100) × (110)]
	(S)-[2(110) × (100)]
(430)	(S)-[4(110) × (100)]
(10,8,7)	(S)-[7(111) × (310)]

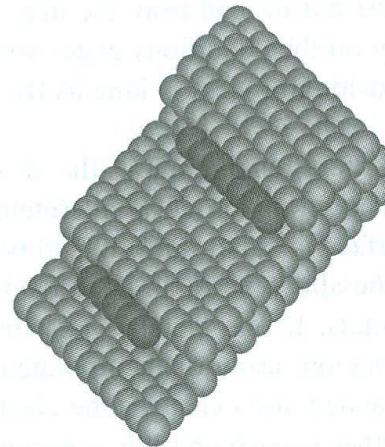
Bimetallic surfaces

Unique properties of a surface composed of two metals

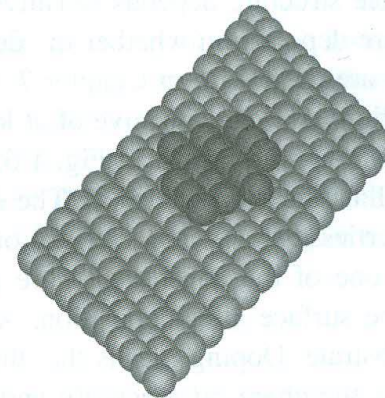


(a)

(b)



(c)



(d)

Figure 1.6 Four limiting cases of the structure of a bimetallic surface prepared by metal-on-metal adsorption: (a) the formation of an intermetallic compound with a definite stoichiometry; (b) random absorption of a miscible metal; (c) segregation of an immiscible metal to the step edges; (d) segregation of an immiscible metal into islands

Oxide and compound semiconductor surfaces

Insulator oxides (> 6 eV band gap): SiO_2 , Al_2O_3 , MgO

Conductor or semiconductor oxides (< 4 eV): CeO_2 , In_2O_3 , SnO_2 , ZnO

Ionic crystals

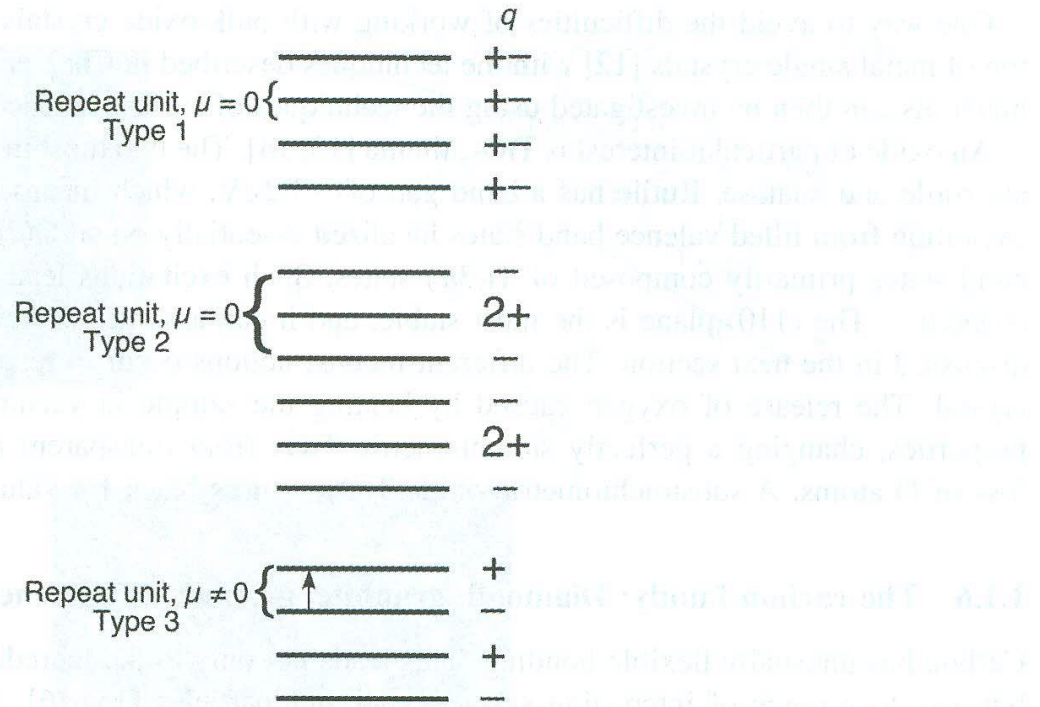


Figure 1.7 Three types of planes formed by ionic crystals. q , ionic charge in layer; μ electric dipole moment associated with the lattice repeat unit.

TABLE 6.2.1. Energy Gaps (E_g) of Selected Materials

Substance	E_g (eV)	Substance	E_g (eV)
Ge	0.67	Fe ₂ O ₃	~ 2.3
CuInSe ₂	0.9	CdS	2.42
Si	1.12	ZnSe	2.58
WSe ₂	~ 1.1	WO ₃	2.8
MoSe ₂	~ 1.1	TiO ₂ (rutile)	3.0
InP	1.3	TiO ₂ (anatase)	3.2
GaAs	1.4	ZnO (zincite)	3.2
CdTe	1.50	SrTiO ₃	3.2
CdSe	1.74	SnO ₂	3.5
GaP	2.2	ZnS (zinc blende)	3.54
		C (diamond)	5.4

Carbon family: diamond, graphite, graphene, etc

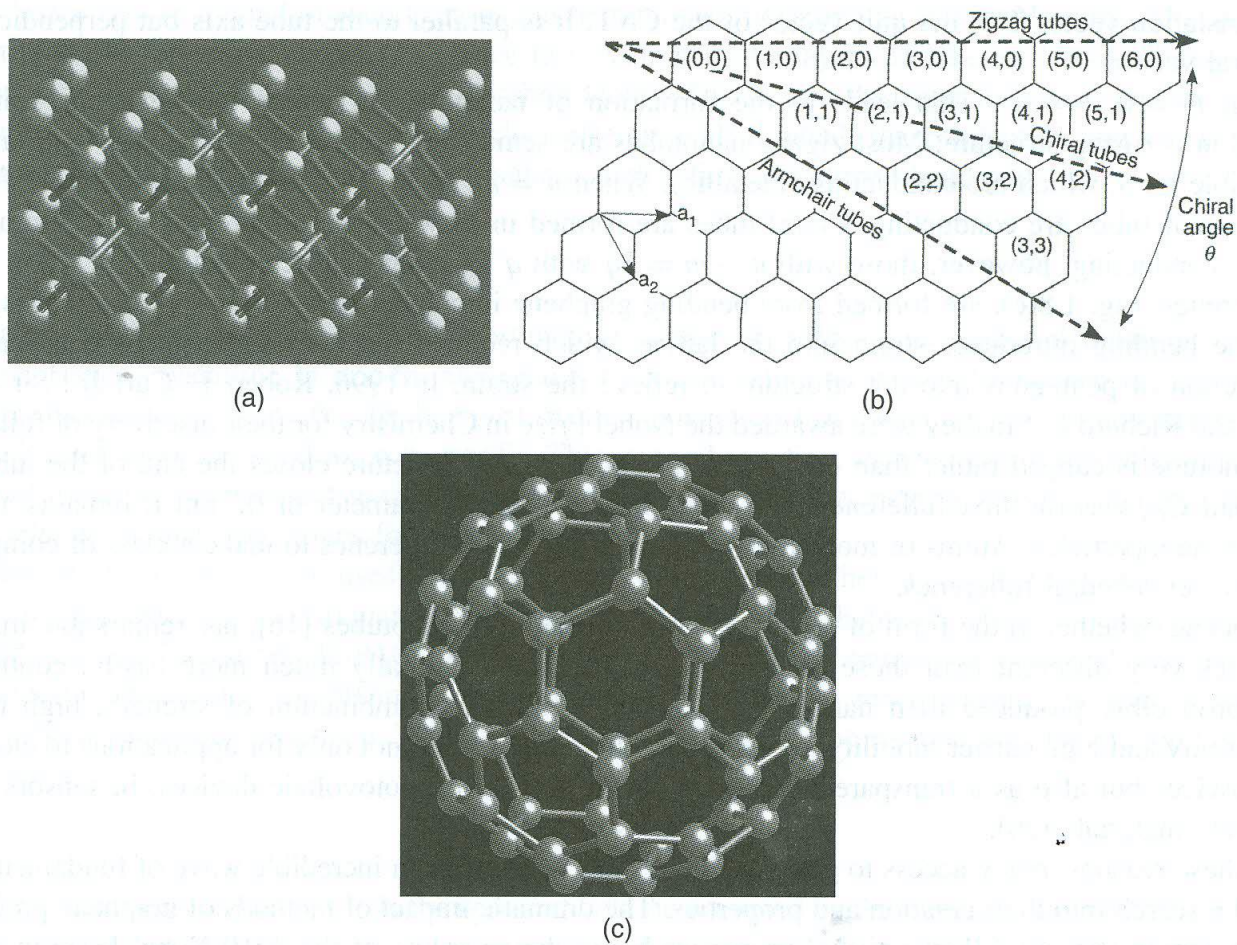


Figure 1.8 (a) A ball and stick model of the diamond lattice with the unreconstructed (111) surface shown at the top. (b) The six-membered ring structure that defines the basal plane of graphite or a graphene sheet. a_1 and a_2 are the surface lattice vectors. When rolled to form a seamless structure, the resulting nanotube has either a zigzag, chiral or armchair configuration depending on the value of the chiral angle. (c) The structure of the fundamental fullerene, that of C₆₀.

Porous solids

Adsorbate structures (Overlayer structures)

Wood's notation: simple but limited

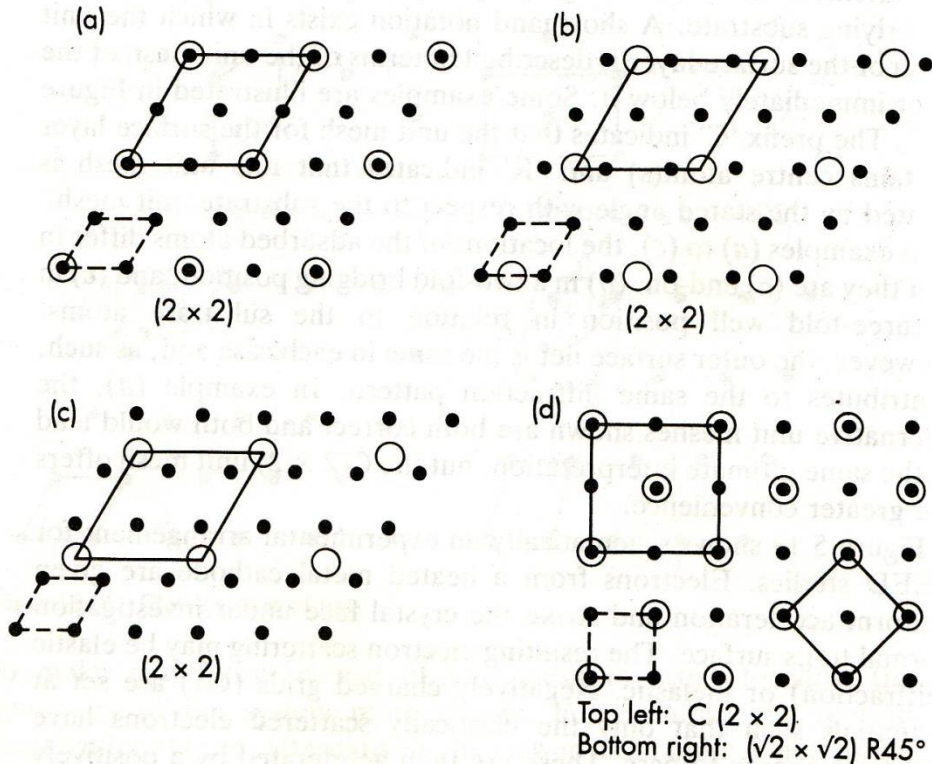


Figure 5.17 Examples and nomenclature of surface layers. Substrate atoms are represented by dots and adatoms by circles. The unit (1×1) mesh of the substrate is shown bottom left

P: primitive

C: centered

R: rotation angle

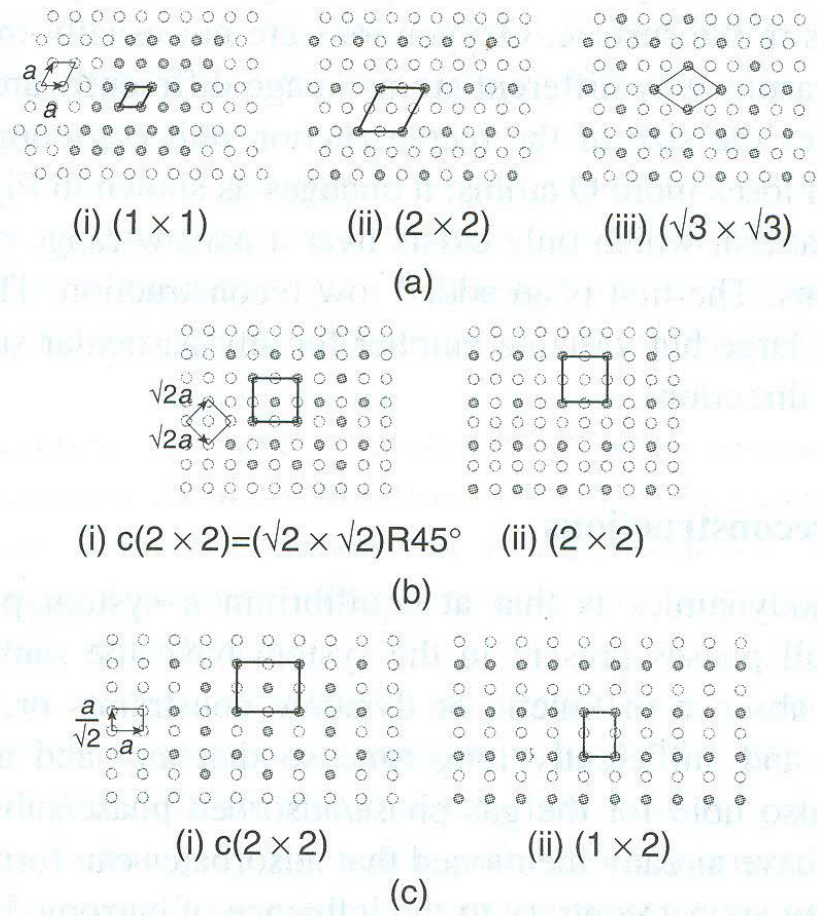


Figure 1.9 Some commonly observed adsorbate structures on low index face-centered cubic (fcc) planes. (a) fcc(111), (i) (1×1) , (ii) (2×2) , (iii) $(\sqrt{3} \times \sqrt{3})$. (b) (i) fcc(100)- $c(2 \times 2)$, (ii) fcc(110)- $c(2 \times 2)$. (c) (i) fcc(100)- (2×2) , (ii) fcc(110)- (1×2) .

Notation of surface structures

- Ideal structure of low-Miller-index surfaces of face-centered cubic (fcc)

Surface unit-cell vectors \mathbf{a}' and \mathbf{b}' can be expressed by bulk \mathbf{a} and \mathbf{b}

$$\begin{aligned}\mathbf{a}' &= m_{11}\mathbf{a} + m_{12}\mathbf{b} \\ \mathbf{b}' &= m_{21}\mathbf{a} + m_{22}\mathbf{b}\end{aligned}\tag{2.4}$$

where the coefficients m_{11} , m_{12} , m_{21} , and m_{22} define a matrix

$$M = \begin{pmatrix} m_{11} & m_{12} \\ m_{21} & m_{22} \end{pmatrix}\tag{2.5}$$

that defines any unit cell unambiguously. For example, for all of the unit cells in Figure 2.8,

$$M = \begin{pmatrix} 1 & 0 \\ 0 & 1 \end{pmatrix}\tag{2.6}$$

Let us consider the surface structure of an adsorbate that has a unit cell twice as long as the substrate unit cell and parallel to it. This structure [e.g., fcc(111)-(2 × 2)] is shown in Figure 2.11. The coefficients of its unit-cell vectors define the matrix

$$M = \begin{pmatrix} 2 & 0 \\ 0 & 2 \end{pmatrix}\tag{2.7}$$

→ superlattice: unit cell different from substrate unit cell: p as primitive, c as centered

Matrix notation: can represent any structure

$$b_1 = m_{11} a_1 + m_{12} a_2 \quad \text{in matrix notation,} \quad b = \mathfrak{M} \cdot a \quad \mathfrak{M} = \begin{pmatrix} m_{11} & m_{12} \\ m_{21} & m_{22} \end{pmatrix}$$

$$b_2 = m_{21} a_1 + m_{22} a_2$$

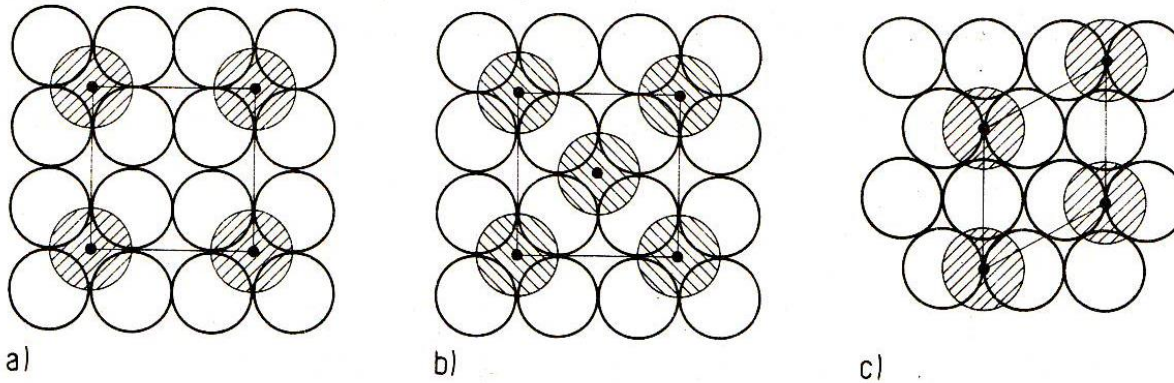
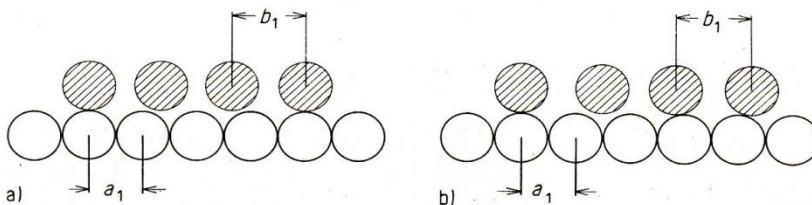


Fig. 9.2. Examples for overlayer structures. a) 2×2 , b) $c(2 \times 2)$, c) $\sqrt{3} \times \sqrt{3} / R 30^\circ$.

$$\mathfrak{M} = \begin{pmatrix} 2 & 0 \\ 0 & 2 \end{pmatrix}, \begin{pmatrix} 1 & 1 \\ -1 & 1 \end{pmatrix} \text{ and } \begin{pmatrix} 1 & 1 \\ -1 & 2 \end{pmatrix}$$

Coherent vs. incoherent structures



$$m a_1 = n b_1$$

$n/m = \text{rational \#} : \text{coherent}$

$\text{irrational \#} : \text{incoherent}$

- Surface structure of adsorbate (superlattice)

(1 x 1): surface atoms identical to the bulk unit cell → substrate structure
 e.g., Pt(111)-(1 x 1)
 (= fcc(111)-(1 x 1))

R: rotation angle

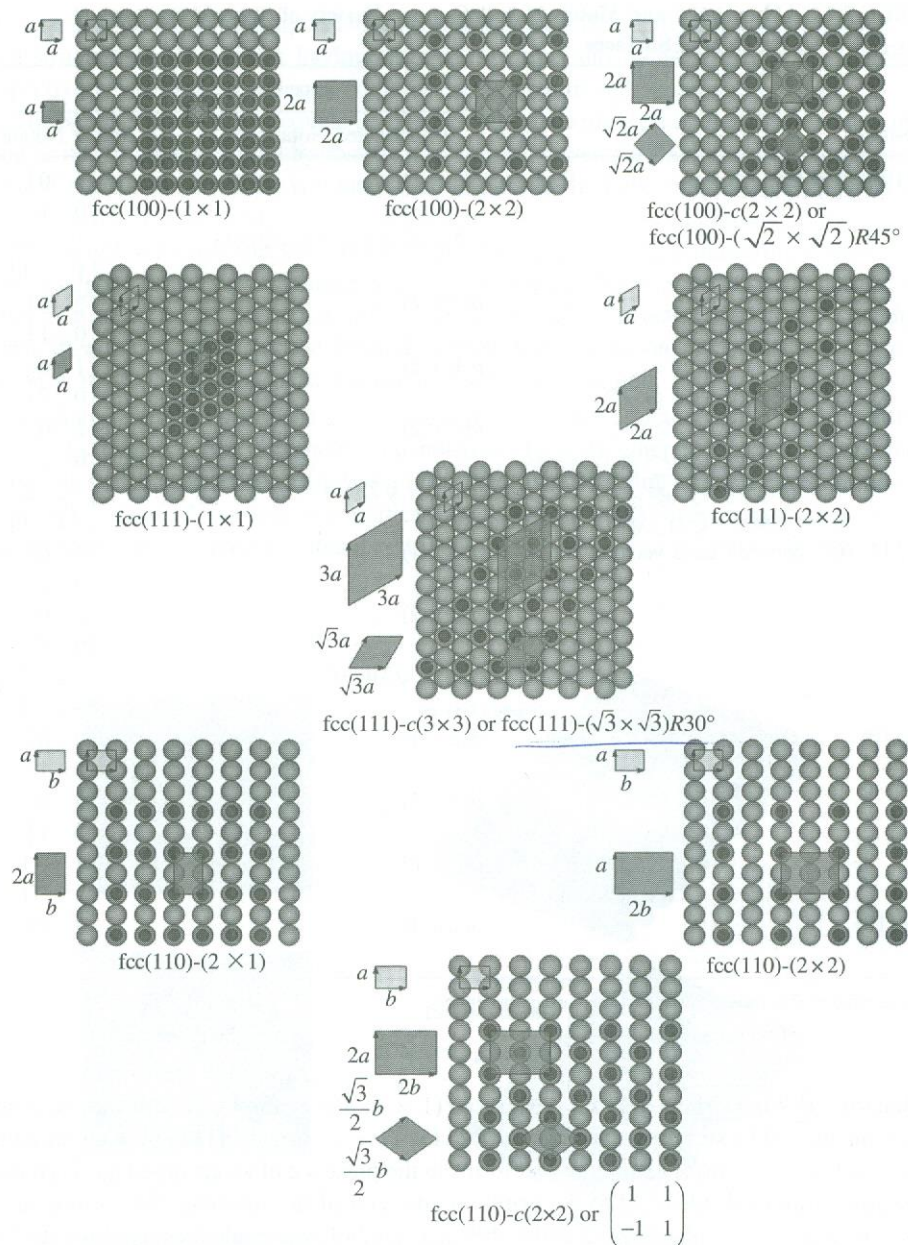


Figure 2.11. Commonly observed unit cells of adsorbate surface structures on fcc(100), (110), and (111) surfaces. (See color insert.)

TABLE 2.1 Abbreviated and Matrix Notations for a Variety of Superlattices on Low-Miller-Index Crystal Surfaces

Substrate	Superlattice Unit Cell	
	Abbreviated Notation ^a	Matrix Notation
fcc(100), bcc(100)	$p(1 \times 1)$	$\begin{vmatrix} 1 & 0 \\ 0 & 1 \end{vmatrix}$
	$c(2 \times 2) = (2\sqrt{2} \times \sqrt{2})R45^\circ$	$\begin{vmatrix} 1 & -1 \\ 1 & 1 \end{vmatrix}$
	$p(2 \times 1)$	$\begin{vmatrix} 2 & 0 \\ 0 & 1 \end{vmatrix}$
	$p(1 \times 2)$	$\begin{vmatrix} 1 & 0 \\ 0 & 2 \end{vmatrix}$
	$p(2 \times 2)$	$\begin{vmatrix} 2 & 0 \\ 0 & 2 \end{vmatrix}$
fcc(111) (60° between basis vectors)	$(2\sqrt{2} \times \sqrt{2})R45^\circ$	$\begin{vmatrix} 2 & 2 \\ -1 & 1 \end{vmatrix}$
	$p(2 \times 1)$	$\begin{vmatrix} 2 & 0 \\ 0 & 1 \end{vmatrix}$
	$p(2 \times 2)$	$\begin{vmatrix} 2 & 0 \\ 0 & 2 \end{vmatrix}$
	$(\sqrt{3} \times \sqrt{3})R30^\circ$	$\begin{vmatrix} 2 & 2 \\ -1 & 2 \end{vmatrix}$
fcc(110)	$p(2 \times 1)$	$\begin{vmatrix} 2 & 0 \\ 0 & 1 \end{vmatrix}$
	$p(3 \times 1)$	$\begin{vmatrix} 3 & 0 \\ 0 & 1 \end{vmatrix}$
	$c(2 \times 2)$	$\begin{vmatrix} 1 & -1 \\ 1 & 1 \end{vmatrix}$
bcc(110)	$p(2 \times 1)$	$\begin{vmatrix} 2 & 0 \\ 0 & 1 \end{vmatrix}$



^aThe parameter R is the orientation of the surface structures.

- Adsorption of atoms (e.g., Na, S, Cl): high coordination surface sites on metal surfaces
- Smaller atomic adsorbates (H, C, N, O): high coordination + penetration within substrate

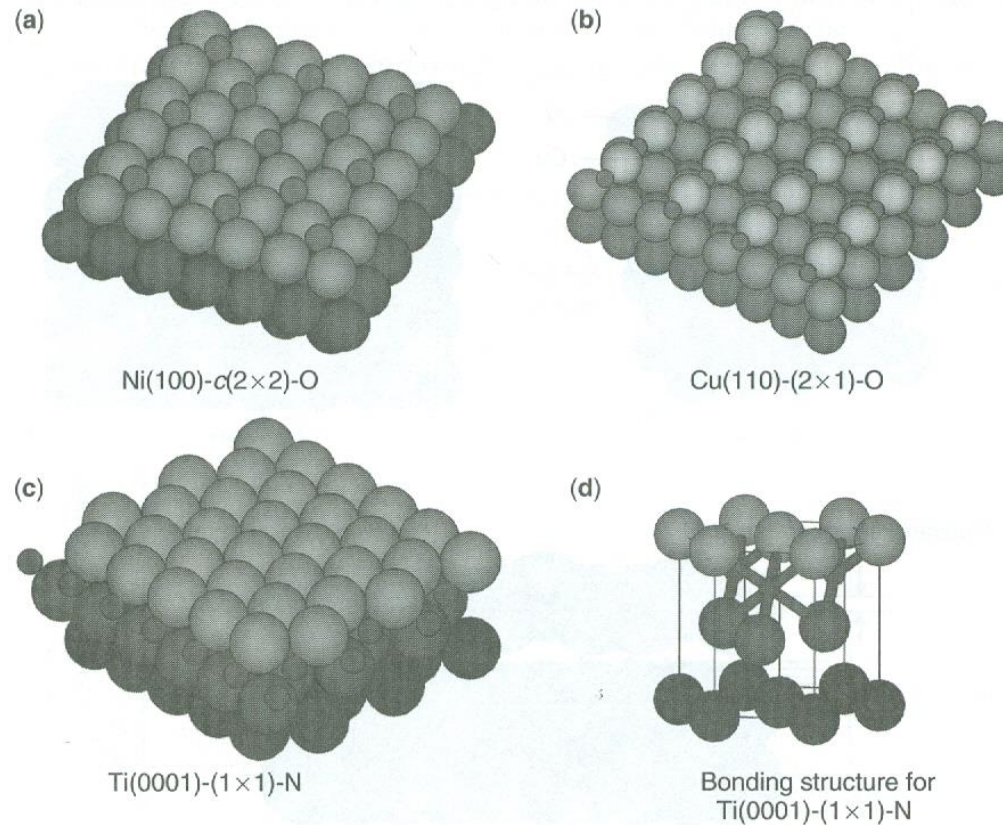


Figure 2.26. (a) The O surface structure on Ni(100) [23]; (b) the O chemisorption induced surface structure on Cu(110) [23]; (c) the N surface structure on Ti(0001) [24]; (d) the bonding structure for N on Ti (0001). All of these structures were obtained by LEED surface crystallography. (See color insert.)

Relaxation

- Relaxation: contraction of the interlayer distance at a clean surface between the first and second layer of atoms

When atoms or molecules adsorb, the surface atoms again relocate to optimize the strength of the adsorption-substrate bond

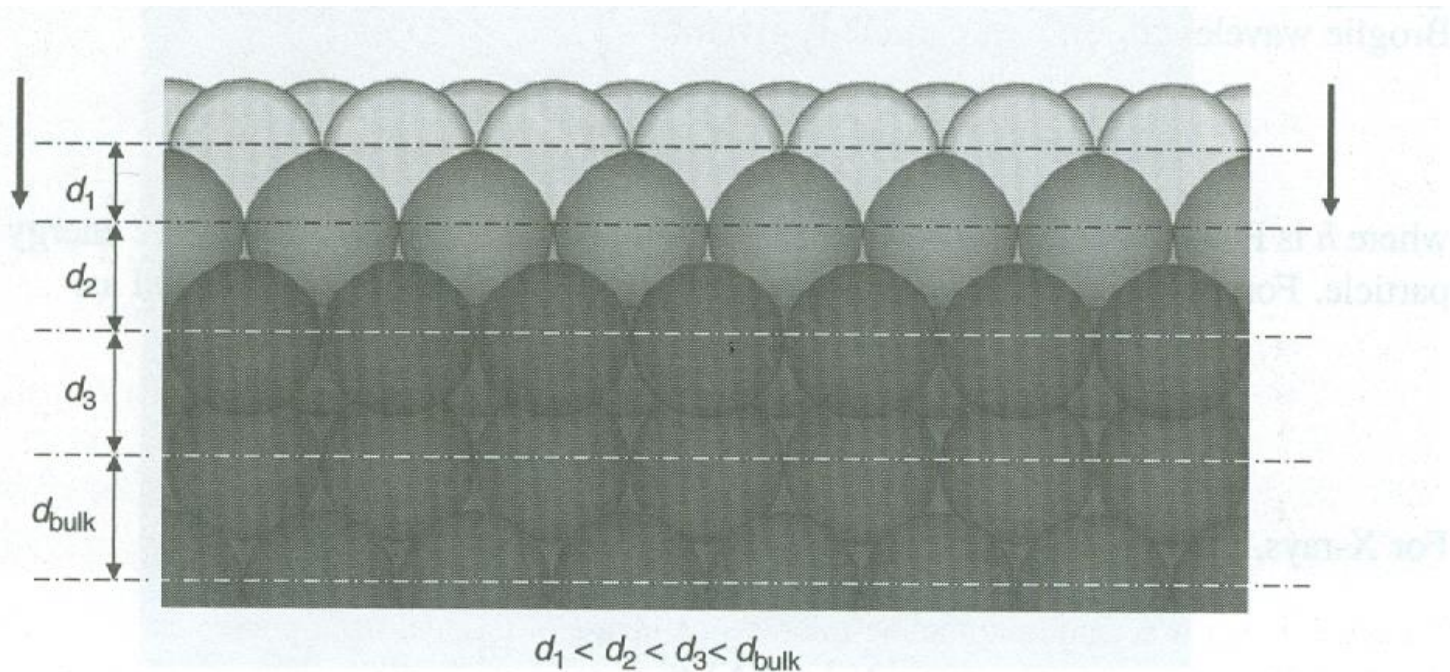
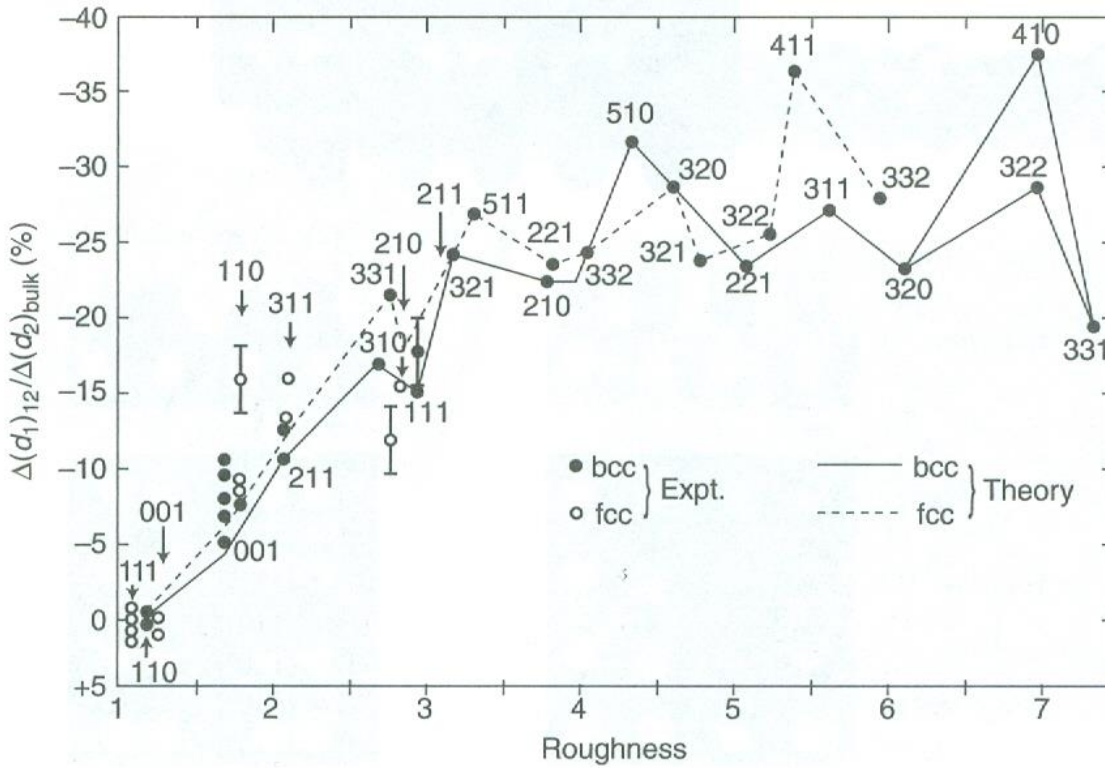


Figure 2.6. Schematic representation of the contraction in interlayer spacing usually observed at clean solid surfaces.

- Bond-length contraction or relaxation: in vacuum, all surface relax \rightarrow reduced spacing between the 1st and 2nd atomic layers

The lower atomic packing/density, the larger the inward contraction



cf.
Nano-segregated surface:
Markovic

Figure 2.14. Contraction of interlayer spacing as a function of surface roughness (defined as 1/packing density) for several fcc and bcc metal surfaces. The points indicate experimental data, and the lines are theoretical fits [4].

Reconstruction

- The forces that lead to surface relaxation → reconstruction of surface layer

e.g., dangling bonds in semiconductor

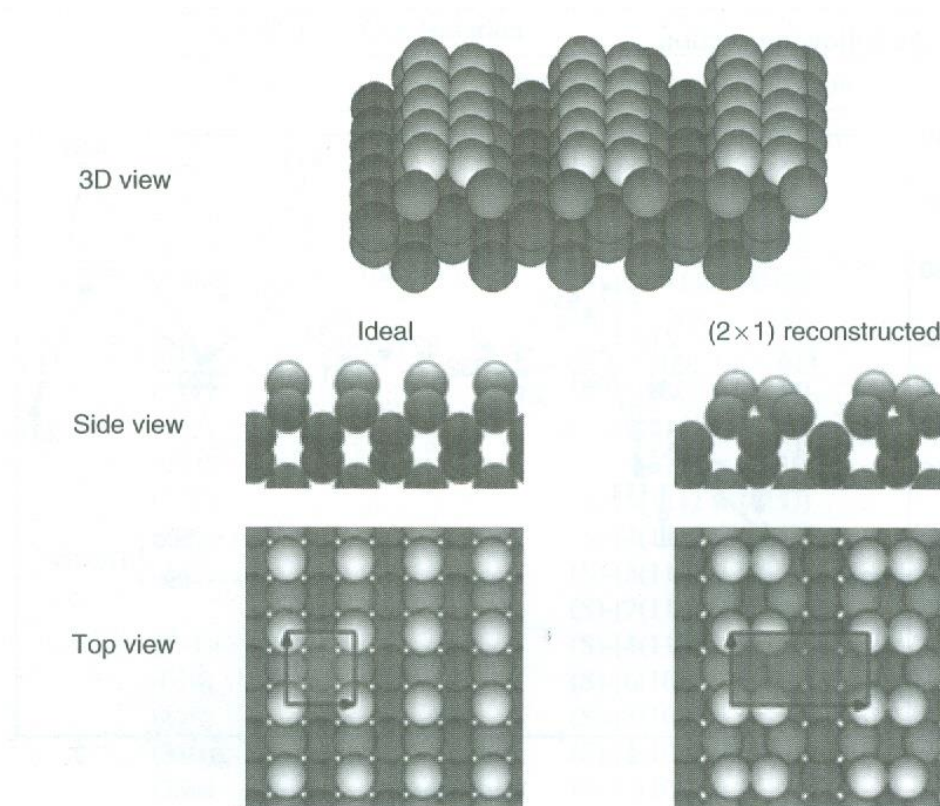
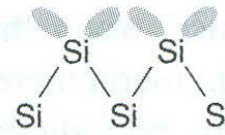
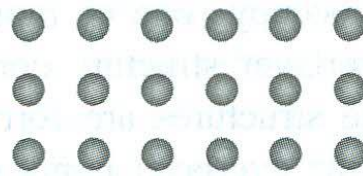


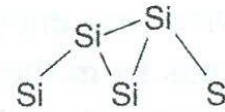
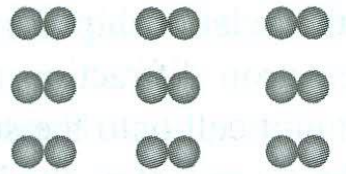
Figure 2.15. The reconstructed Si(100) crystal face as obtained by LEED surface crystallography. The upper layer is indicated by a lighter color. Note that surface relaxation extends to three atomic layers into the bulk [8].

Top View

Side View



(a)



(b)

Figure 1.10 The $\text{Si}(100)-(2 \times 1)$ reconstruction: (a) unreconstructed clean $\text{Si}(100)-(1 \times 1)$; (b) reconstructed clean $\text{Si}(100)-(2 \times 1)$.

- Reconstruction in metal surfaces: several % in Pt, Au, Ir and so on

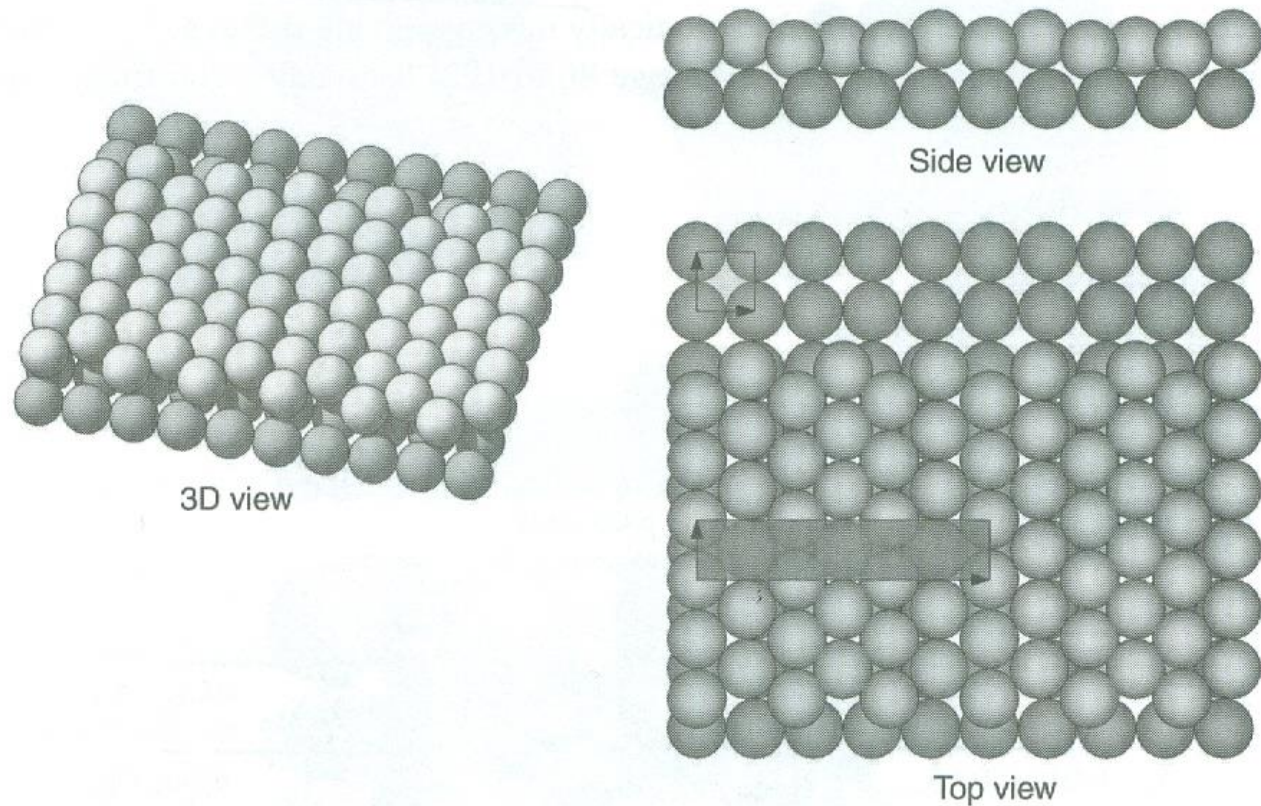


Figure 2.17. The structure of the reconstructed Ir(100) crystal face obtained from LEED surface crystallography. The first layer is indicated by a lighter color. Hexagonal packing in the surface layer induces buckling. The second layer retains its square unit cell. (See color insert.)

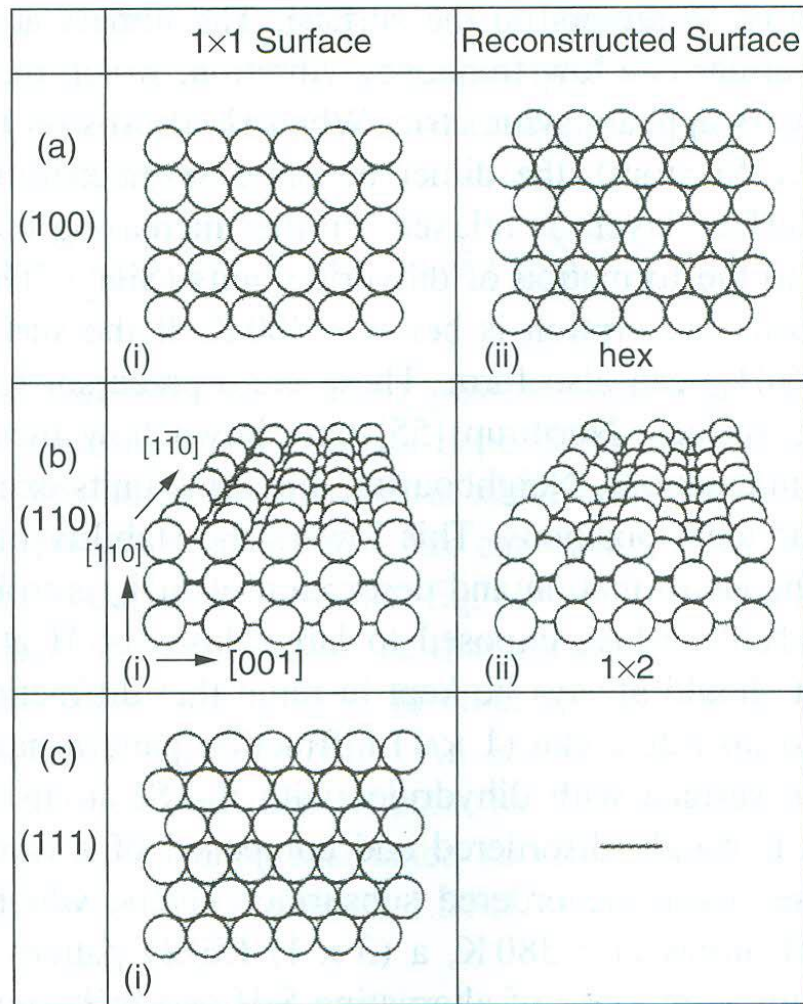


Figure 1.13 Reconstructed and unreconstructed surfaces for the three low index planes of Pt: (a) (100) plane, (i) (1 × 1) unreconstructed surface, (ii) quasi-hexagonal (hex) reconstructed surface; (b) (110) plane, (i) (1 × 1) unreconstructed surface, (ii) missing row (1 × 2) reconstructed surface; (c) (111) plane, (i) (1 × 1) unreconstructed surface (Pt(111) is stable against reconstruction). Reproduced from R. Imbihl and G. Ertl, *Chem. Rev.* 95, 697. © (1995), with permission from the American Chemical Society.

- Reconstruction of high-Miller-index surfaces: roughening transition

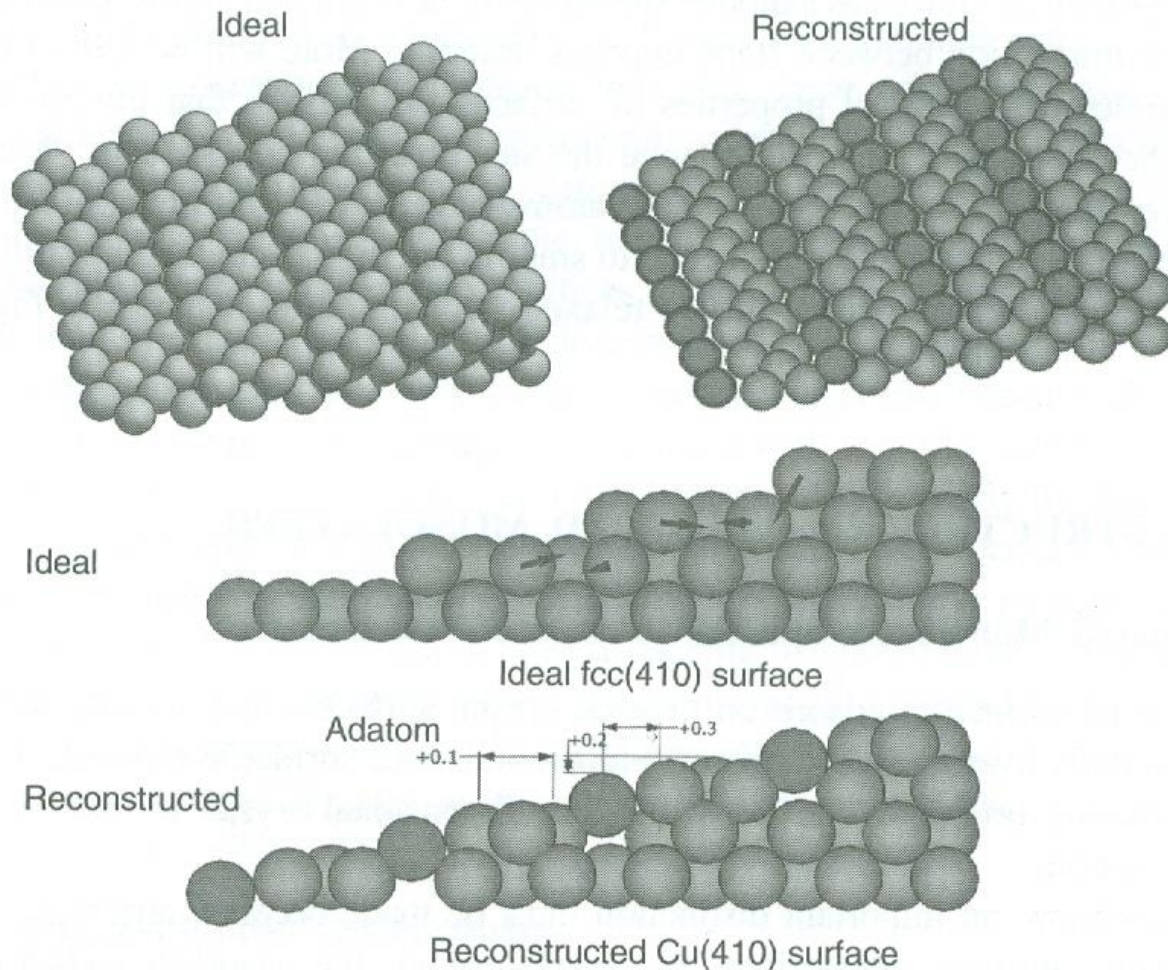


Figure 2.20. Relaxation at a Cu(410) stepped surface [21]. The relative displacements (in Angstrom) of atoms are shown in the side view of the bulk surface. Atoms in the first row at the each step become adatoms that are pointed out in the side view of the reconstructed surface. (See color insert.)

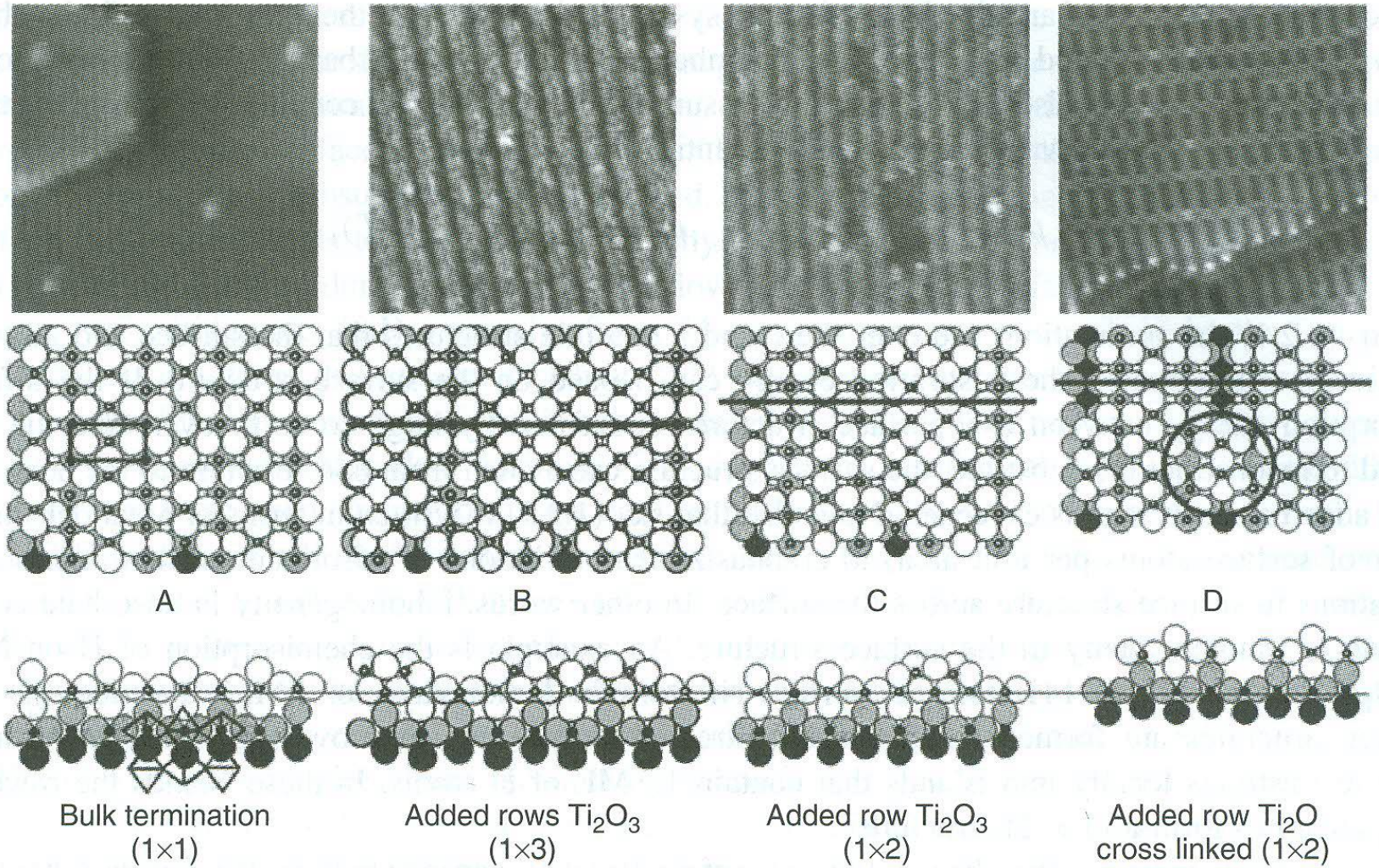


Figure 1.11 The surface structures observed on $\text{TiO}_2(110)$ as a function of increasing bulk reduction of the crystal. Upper panels are scanning tunnelling microscope images with 20 nm scan size. The lower two panels display the proposed surface structures. Reproduced from M. Bowker, *Curr. Opin. Solid State Mater. Sci.* 10, 153. (2006) with permission from Elsevier.

Adsorbate induced reconstructions

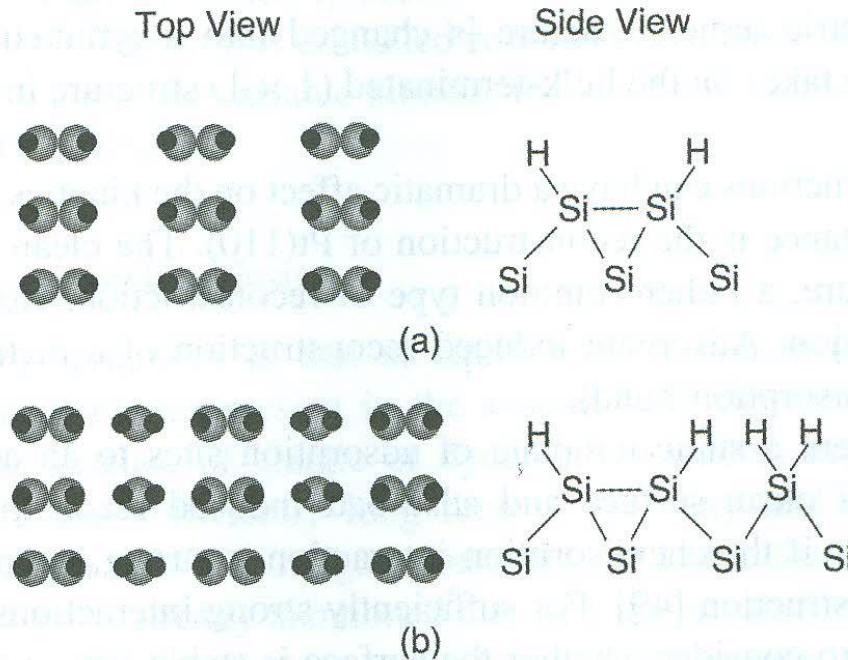


Figure 1.12 The adsorption of H on to Si(100): (a) $\text{Si}(100)-(2 \times 1):\text{H}$, $\theta(\text{H}) = 1 \text{ ML}$; (b) $\text{Si}(100)-(3 \times 1):\text{H}$, $\theta(\text{H}) = 1.33 \text{ ML}$. Note: the structures obtained from the adsorption of hydrogen atoms on to Si(100) are a function of the hydrogen coverage, $\theta(\text{H})$. $1 \text{ ML} = 1 \text{ monolayer}$ as defined by 1 hydrogen atom per surface silicon atom.

Chiral surfaces

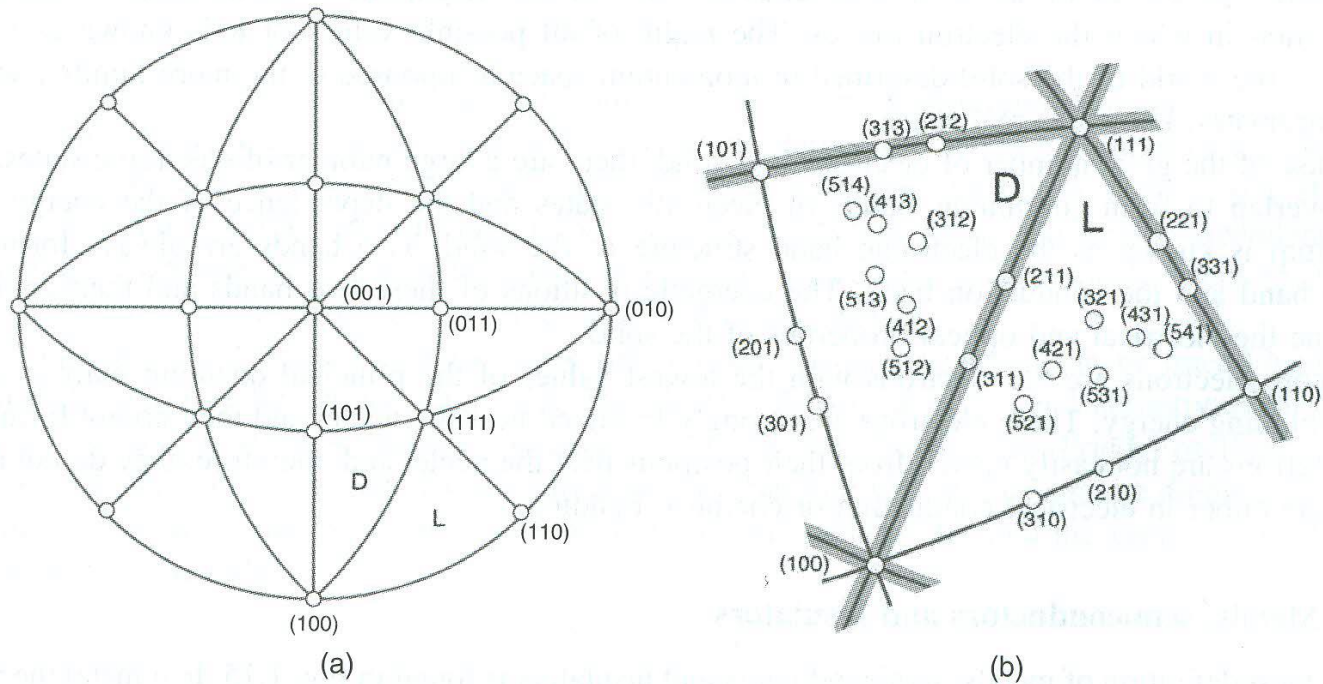


Figure 1.14 Stereogram projected on (001) showing the mirror zones relevant to primitive fcc, bcc and simple cubic crystal surfaces. Note that right-handed axes are used. The chiralities of two triangles are labelled D and L according to symmetry-based convention of Pratt et al. [63]. Reproduced from S.J. Pratt, S.J. Jenkins, D.A. King, *Surf. Sci.*, 585, L159. © (2005), with permission from Elsevier.

Electronic structure of solids

Metals, semiconductors and insulators

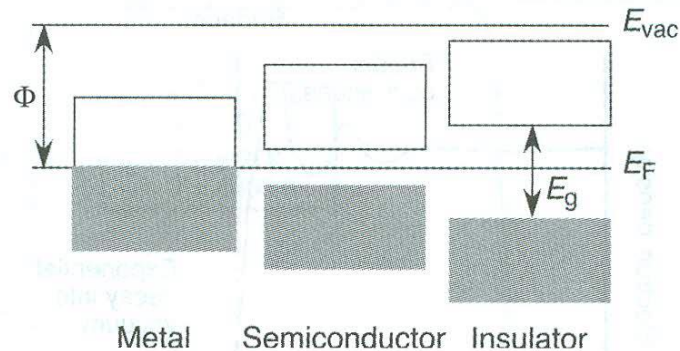


Figure 1.15 Fermi energies, vacuum energies and work functions in a metal, a semiconductor and an insulator. The presence and size of a gap between electronic states at the Fermi energy, E_F , determines whether a material is a metal, semiconductor or insulator. E_g , band gap; Φ work function equal to the difference between E_F and the vacuum energy, E_{vac} .

Fermi level (E_F): the energy of the highest occupied electronic state (at 0 K)

At higher T, e^-h^+ pair formation

Vacuum energy (E_{vac}): the energy of a material and an e^- at infinite separation

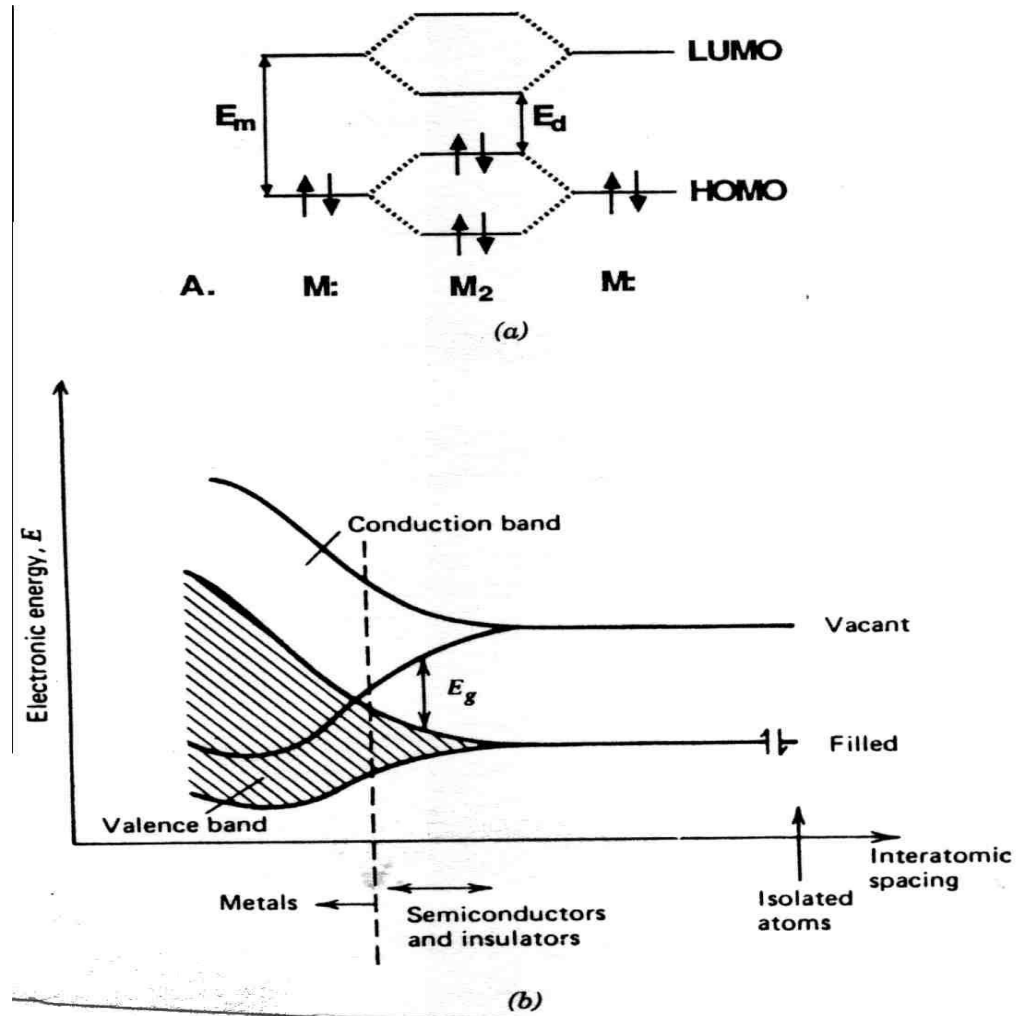
Work function (Φ):

e : the elementary charge

→ minimum energy to remove one e^- from the material to infinity at 0 K.

actual min. ionization energy is great than Φ due to no state at E_F for SC & insulator

Band model



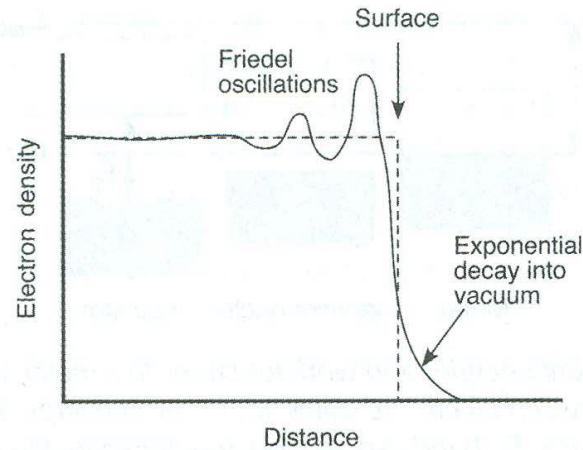


Figure 1.16 Friedel oscillations: the electron density near the surface oscillates before decaying exponentially into the vacuum

Dependence of the work function (Φ) on surface properties

→ e^- density does not end abruptly at the surface (Fig.1.16), instead, it oscillates near the surface (Friedel oscillation)

probability that an electronic level at energy E is occupied by an electron at thermal equilibrium $f(E)$ → Fermi-Dirac distribution function

$$f(E) = \frac{1}{1 + \exp [(E - E_F)/kT]}$$

Fermi level E_F ; value of E for which $f(E) = 1/2$ (equally probable that a level is occupied or vacant)

At $T = 0$, all levels below E_F ($E < E_F$) are occupied ($f(E) \rightarrow 1$); all levels $E > E_F$ vacant

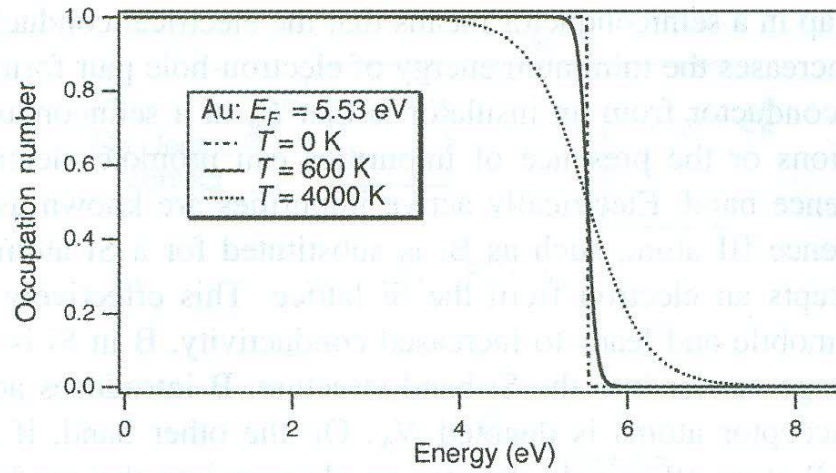


Figure 1.17 Fermi-Dirac distribution for gold at three different temperatures, T , E_F , Fermi energy.

Band gap (E_g),

$$E_g = E_c - E_v$$

Fermi level of intrinsic semiconductor

Energy levels at metal interfaces

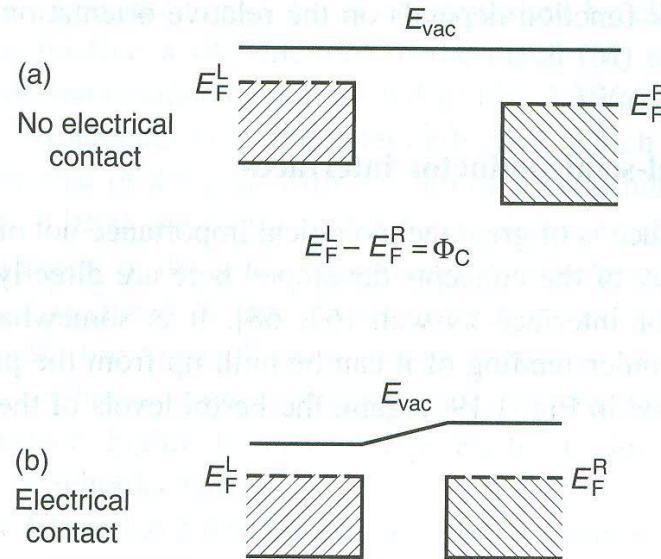
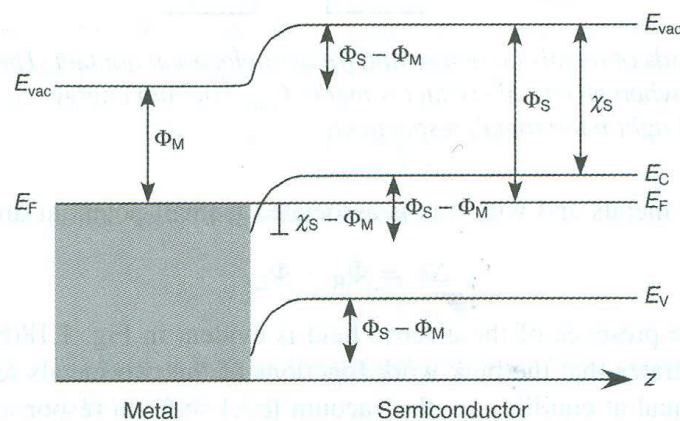


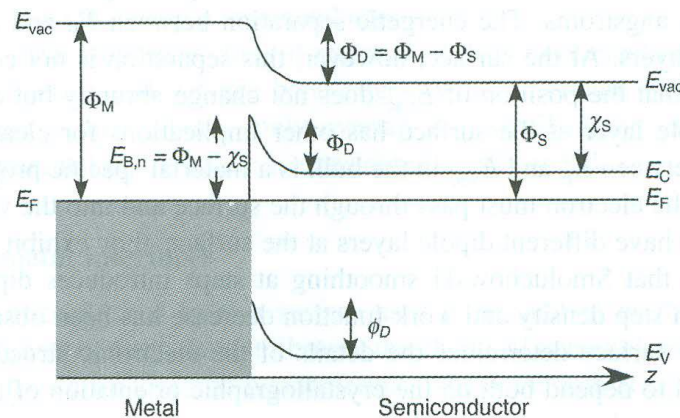
Figure 1.18 Electronic bands of metals (a) before and (b) after electrical contact. The Fermi energies of the two metals align at equilibrium when electrical contact is made. E_{vac} , vacuum energy; E_F , Fermi energy; subscripts L and R refer to left-hand and right-hand metal, respectively.

Electron flow: R to L

Energy levels at metal-semiconductor interfaces



(a)



(b)

Figure 1.19 Band bending in an *n*-type semiconductor at a heterojunction with a metal. (a) Ohmic contact ($\Phi_S > \Phi_M$). (b) Blocking contact (Schottky barrier, $\Phi_S < \Phi_M$). The energy of the bands is plotted as a function of distance z in a direction normal to the surface. Φ_S , Φ_M work function of the semiconductor and of the metal, respectively; E_{vac} , vacuum energy; E_C , energy of the conduction band minimum; E_F , Fermi energy; E_V energy of the valence band maximum; E_g band gap. Reproduced from S. Elliott, *The Physics and Chemistry of Solids*, John Wiley, New York. © (1998), with permission from John Wiley & Sons, Ltd.

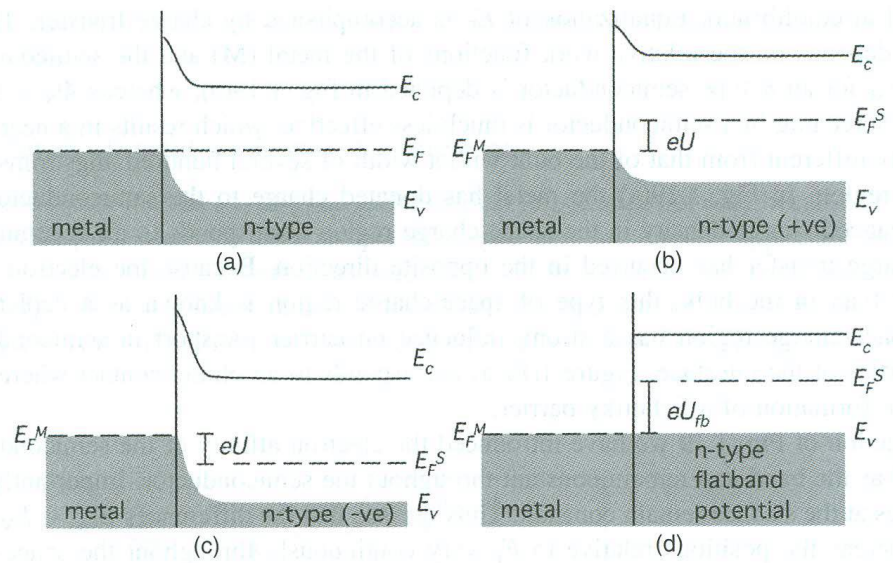


Figure 1.20 The electrochemical potential and the effects of an applied voltage on a metal/semiconductor interface. (a) No applied bias. (b) Forward bias. (c) Reverse bias. (d) Biased at the flatband potential, U_{fb} . E_C , energy of the conduction band minimum; E_F , Fermi energy; E_V , energy of the valence band maximum; superscripts M and S refer to the metal and the semiconductor, respectively.

Surface electronic states

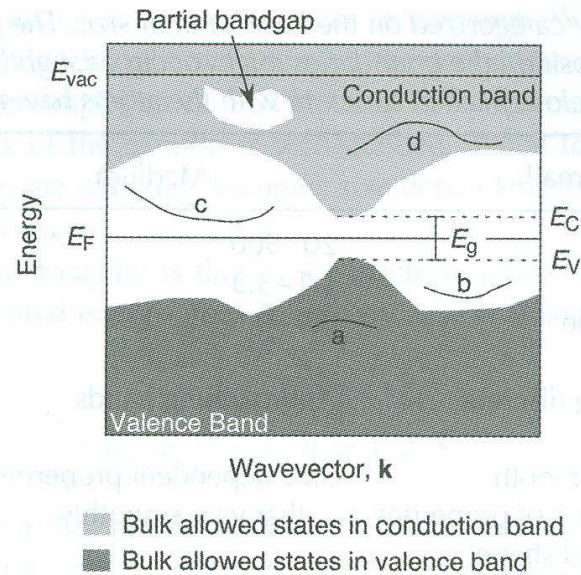


Figure 1.21 — The band structure of a semiconductor, including an occupied surface resonance (a), an occupied surface state (b), a normally unoccupied surface state (c), and a normally unoccupied surface resonance (d). E_{vac} , vacuum energy; E_F , Fermi energy; E_V , energy of the valence band maximum; E_C , the conduction band minimum.

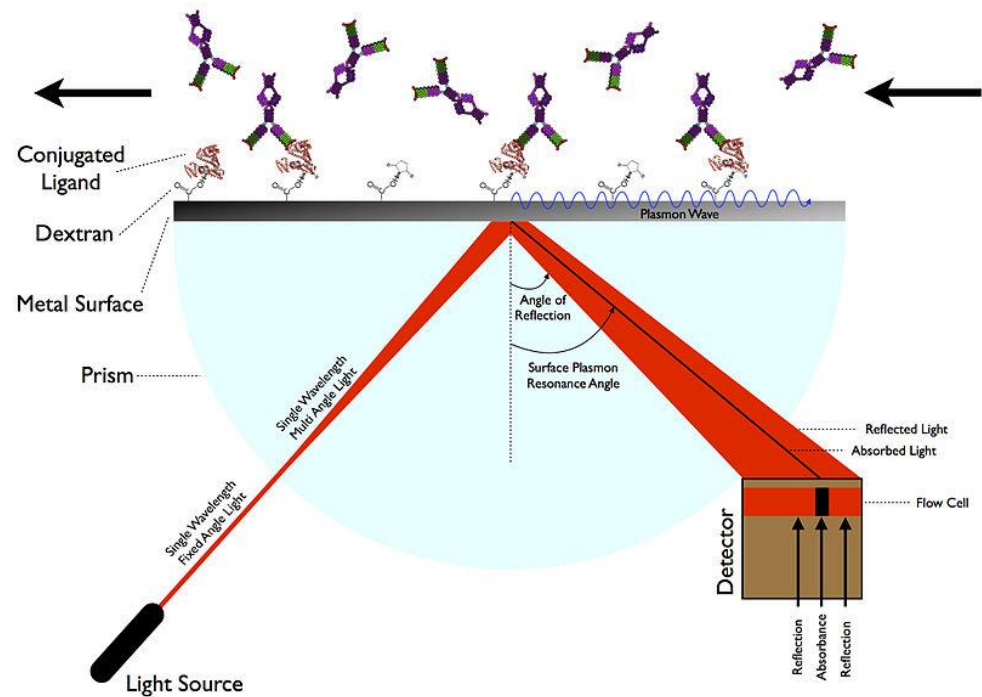
Size effects in nanoscale systems

Table 1.2 Clusters can be roughly categorized on the basis of their size. The properties of clusters depend on size. For clusters of different composition the boundaries might occur as slightly different values. The diameter is calculated on the assumption of a close packed structure with the atoms having the size of a Na atom

	Small	Medium	Large
Atoms (N)	2–20	20–500	500– 10^6
Diameter/nm	≤ 1.1	1.1–3.3	3.3–100
Surface/Bulk (N_s/N)	Not separable	0.9–0.5	$\leq 0.5 \sim 0.2$ for $N = 3\,000$ $\ll 1$ for $N \geq 10^5$
Electronic states	Approaching discrete	Approaching bands	Moving toward bulk behaviour
Size dependence	No simple, smooth dependence of properties on size and shape	Size dependent properties that vary smoothly	Quantum size effects may still be important but properties approaching bulk values

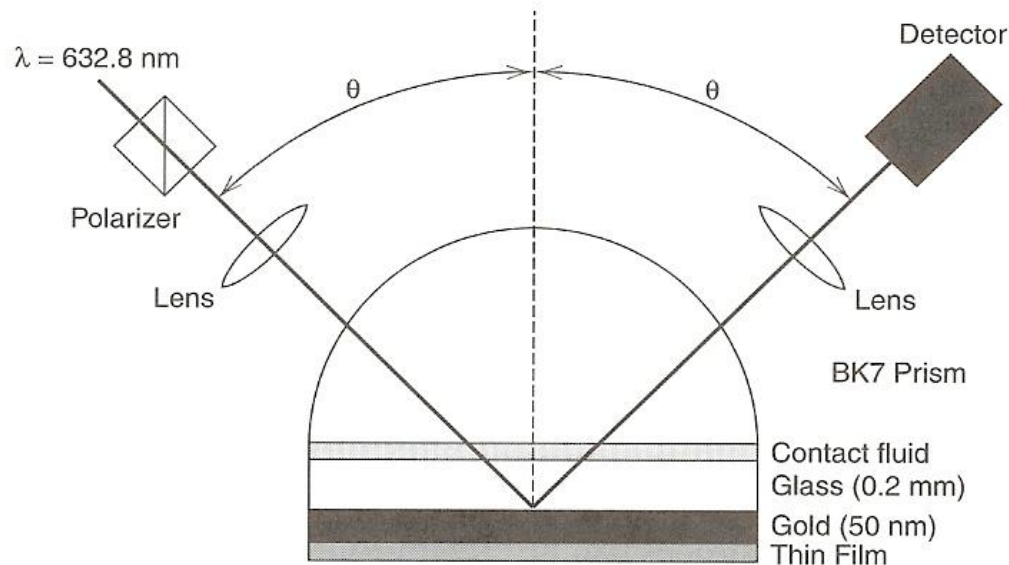
Vibrations of solids

Surface plasmon resonance (SPR)



Surface plasmon resonance (SPR) is the collective oscillation of valence electron in a solid stimulated by incident light. The resonance condition is established when the frequency of light photons matches the natural frequency of surface electrons oscillating against the restoring force of positive nuclei. SPR in nanometer-sized structures is called **localized surface plasmon resonance**. SPR is the basis of many standard tools for measuring adsorption of material onto planar metal (typically gold and silver) surfaces or onto the surface of metal nanoparticles. It is the fundamental principle behind many color-based biosensor applications and different lab-on-a-chip sensors. (from Wikipedia)

Surface plasmon



플라스몬(plasmon)이란 금속 내의 자유전자가 집단적으로 진동하는 유사 입자를 말한다. 금속의 나노 입자에서는 플라스몬이 표면에 국부적으로 존재하기 때문에 표면 플라스몬(surface plasmon)이라 부르기도 한다. 그 중에서도 금속 나노 입자에서는 가시~근적외선 대역 빛의 전기장과 플라스몬이 짝지어지면서 광흡수가 일어나 선명한 색을 띠게 된다. (이 경우, 플라스몬과 광자가 결합되어 생성하는 또다른 유사 입자를 플라스마 폴라리톤이라고 한다.) 이 현상을 표면 플라스몬 공명(surface plasmon resonance)이라 하며, 국소적으로 매우 증가된 전기장을 발생시킨다. (위키백과)